European Journal of Medicinal Chemistry 208 (2020) 112699

Contents lists available at ScienceDirect

European Journal of Medicinal Chemistry

journal homepage: http://www.elsevier.com/locate/ejmech

New one-pot synthesis of anti-tuberculosis compounds inspired on isoniazid

Diego G. Ghiano [a], Alejandro Recio-Balsells [a], Ana Bortolotti [b, 1], Lucas A. Defelipe [c, d], Adrián Turjanski [c, d], Héctor R. Morbidoni [b, e], Guillermo R. Labadie [a, f, *]

[a] Instituto de Química Rosario, UNR, CONICET, Suipacha 531, S2002LRK, Rosario, Argentina
[b] Laboratorio de Microbiología Molecular, Facultad de Ciencias Médicas, Universidad Nacional de Rosario, Santa Fe 3100, S2002KTR, Rosario, Argentina
[c] IQUIBICEN-CONICET, Ciudad Universitaria, Pabellón 2, C1428EHA, Ciudad de Buenos Aires, Argentina
[d] Departamento de Química Biológica, Facultad de Ciencias Exactas y Naturales, Universidad de Buenos Aires, Ciudad Universitaria, Pabellón 2, C1428EHA, Ciudad de Buenos Aires, Argentina
[e] Consejo de Investigaciones Científicas, Universidad Nacional de Rosario, Argentina
[f] Departamento de Química Orgánica, Facultad de Ciencias Bioquímicas y Farmacéuticas, Universidad Nacional de Rosario, Suipacha 531, S2002LRK, Rosario, Argentina

ARTICLE INFO

Article history:
Received 10 February 2020
Received in revised form
22 July 2020
Accepted 25 July 2020
Available online 22 August 2020

Keywords:
Aza-Michael
Tuberculosis
InhA
One-pot
Docking
Chemoinformatics

ABSTRACT

A library of thirty N-substituted tosyl N'-acryl-hydrazones was prepared with p-toluenesulfonyl hydrazide, methyl propiolate and different aldehydes in a one-pot synthesis *via* an aza-Michael reaction. The scope of the reaction was studied, including aliphatic, isoprenylic, aromatic and carbocyclic aldehydes. The prepared collection was tested against *Mycobacterium tuberculosis* H37Rv. Nine analogs of the collection showed Minimum Inhibitory Concentration $\leq$10 μM, of which the most active members (MIC of 1.25 μM) were exclusively *E* isomers. In order to validate the mechanism of action of the most active acrylates, we tested their activity on a *M. tuberculosis* InhA over-expressing strain obtaining MIC that consistently doubled those obtained on the wild type strain.

Additionally, the binding mode of those analogs on *M. tuberculosis* InhA was investigated by docking simulations. The results displayed a hydrogen bond interaction between the sulfonamide and Ile194 and the carbonyl of the methyl ester with Tyr 158 (both critical residues in the interaction with the fatty acyl chain substrate), where the main differences on the binding mode relays on the hydrophobicity of the nitrogen substituent. Additionally, chemoinformatic analysis was performed to evaluate *in silico* possible cytotoxicity risk and ADME-Tox profile.

Based on their simple preparation and interesting antimycobacterial activity profile, the newly prepared aza-acrylates are promising candidates for antitubercular drug development.

© 2020 Elsevier Masson SAS. All rights reserved.

1. Introduction

Tuberculosis (TB) remains a major infectious disease and is a great cause of death throughout the world. The World Health Organization (WHO) estimated 10.0 million new TB cases and 1.6 million deaths in 2017 (including 300.000 deaths caused in HIV-positive people) [1]. In addition, multidrug-resistant tuberculosis (MDR-TB, resistant to Isoniazid and Rifampicin) is becoming more common [2] with 458.000 new cases in the World in 2017 [1]. It is estimated that about 8.5% of these cases were caused by extensively-drug-resistant *M. tuberculosis* (XDR-TB), showing additional resistance to at least a fluoroquinolone and one injectable drug (amikacin, kanamycin or capreomycin) [1,3]. For patients affected by XDR-TB, the therapeutic efficacy of standard treatments is quite limited. Additionally, the emergence of "Totally drug-resistant" *M. tuberculosis* strains that have a low rate of successful treatment is becoming a health threat in certain regions of the planet [4].

The common treatment for TB consists of a cocktail of four

* Corresponding author. Instituto de Química Rosario, UNR, CONICET, Suipacha 531, S2002LRK, Rosario, Argentina.
E-mail address: labadie@iquir-conicet.gov.ar (G.R. Labadie).
[1] Current address: Departamento de Microbiología, Facultad de Ciencias Bioquímicas y Farmacéuticas, Suipacha 531, Universidad Nacional de Rosario, Argentine National Research Council (CONICET), Rosario, Argentina.

https://doi.org/10.1016/j.ejmech.2020.112699
0223-5234/© 2020 Elsevier Masson SAS. All rights reserved.

drugs: isoniazid, rifampicin, ethambutol and pyrazinamide over a 6- to 9-month period. Also, anti-tuberculosis drugs induce hepatotoxicity (ATDH), causing substantial morbidity and mortality and diminishing treatment effectiveness. Side effects are the main reasons for the non-adherence to the current treatment, reducing the effectiveness and eventually contributing to failure, relapse, or the emergence of drug-resistance [5].

Therefore, there is an urgent need to develop new drugs. New candidates need to be able to shorten and simplify the actual treatment, to improve tolerance, be active against resistant strains (MDR-TB, XDR-TB) and also be compatible with anti-HIV therapies in TB-HIV patients [6].

One of the most effective and specific antituberculosis drugs is Isoniazid (INH). It has been a key chemotherapeutic agent since it was introduced in 1952 [7]. INH is active only on growing tubercle bacilli, not being effective against non-replicating bacilli or under anaerobic conditions [8,9].

INH is a prodrug that is activated by the mycobacterial catalase-peroxidase enzyme KatG [10], producing an isonicotinoyl acyl radical which reacts with NAD/NADH species to give the INH-NADH adduct (Scheme 1). This adduct inhibits the enoyl ACP (Acyl Carrier Protein) reductase (InhA), thus blocking the mycolic acid biosynthesis and affecting the integrity of the cell wall, leading to cell death [11]. Mutations in several genes (*kat*G, *ahp*C, *kas*A, *inh*A) have been described as mediating resistance to INH, however it has been clearly shown that the essential InhA encoded by *inh*A is the true target for the activated INH. Of outmost importance, mutations abrogating the activity of KatG —which are vastly predominant worldwide in clinical strains-prevent the activation of the prodrug into active forms, rendering INH totally inactive [10]. Therefore, new compounds targeting InhA without the need of an activation step are desperately needed to replace INH and combat multidrug-resistant strains of *M. tuberculosis* [12]. Despite its proven applicability and effectivity, INH has yet another major drawback as it produces adverse reactions that include hepatotoxicity and neurotoxicity [13].

In recent years, compounds with structural features based on INH with antituberculosis activity have been developed (Fig. 1) [14–16]. Among those, there are new analogs which introduced substituents over the terminal nitrogen, keeping the isonicotinic portion without modifications (Fig. 1, Compound **A**) [17]. Another approach exchanges the isonicotinic portion with different aromatics substituents (Fig. 1, Compound **B**) [18]. The hydrazone has also been exchanged by a hydrazine that displayed high MIC on *M. tuberculosis* H37Rv, but its IC_{90} on anaerobic and aerobic condition was between 3 and 4 times more active, respectively (Fig. 1, Compound **C**) [19,20]. Alternatively, N-arylsulfonyl derivatives have been prepared as metallo-β-lactamases inhibitors to overcome the resistance mechanisms generated by some bacterial species (Fig. 1. Compound **D**) [21]. Those results encouraged us to develop new compounds structurally related to isoniazid. A detailed look on the reported compounds showed that only few examples of N'-substituted derivatives have been reported and their biological activity has not been explored.

On the other side, tosylhydrazones have shown antibacterial activity and have also been present in analogs with antinociceptive activity [22]. Also, there are tosylhydrazones reported as inhibitors of monoamine oxidase A, a target for anti depressives [23,24], and as acetylcholinesterase inhibitors, a target for Alzheimer's disease treatment [25]. (Fig. 2).

In the present study, we explore the N-substituted tosylhydrazones scaffold (Fig. 2, Compound **E**), structurally related to isoniazid, looking for the design of more effective compounds that would overcome drug resistance and reduce or eliminate adverse effects.

The proposed structure has a new substituent on the secondary nitrogen. This modification will introduce stereoelectronic differences that could contribute to sustain and improve the antimycobacterial activity overcoming known resistant mechanisms related to activation of INH [20].

2. Results and discussions

2.1. Chemistry

Synthetically N-substituted tosylhydrazones scaffold can be prepared by different strategies, but a critical point was the nature of the secondary nitrogen substituent. In order to improve the activity, we looked for potential moieties that contribute to the activity as pharmacophores. We found that hetero-substituted *E*-ethyl acrylate **E** (Scheme 2) have shown moderate antimycobacterial activity [26]. Therefore, combining tosylhydrazones with hetero-substituted *E* acrylates could improve the activity as a hybrid drug [27]. That compound also has the advantage that it can be prepared by an aza-Michael reaction between methyl propiolate **1** and tosylhydrazone anion **2** as is shown in Scheme 2.

Sulfonyl hydrazines are widely used as intermediates for heterocyclic synthesis, such as indazole [28], 1,2,4-triazines [29], 1,2,4,5-tetrazines [30] and H-pyrazolo [5,1a] isoquinolines [31]. The synthesis of the N-substituted acrylates by aza-Michel reaction has been recently explored. One example of that approach involved the reaction of aromatic benzyl hydrazones with ethyl propiolate under basic conditions (DABCO) [32]. Another reported procedure used triphenylphosphine to capture the 1,3-zwitterionic intermediate generated by the reaction of sulfonyl hydrazones with ethyl propiolate [33]. Both reactions were conducted at room temperature and were regioselective, generating only the *E* adduct with moderate to high yields. Similar compounds can also be prepared by Mitsunobu reactions [34] or nucleophilic substitution of alkylhalides [35].

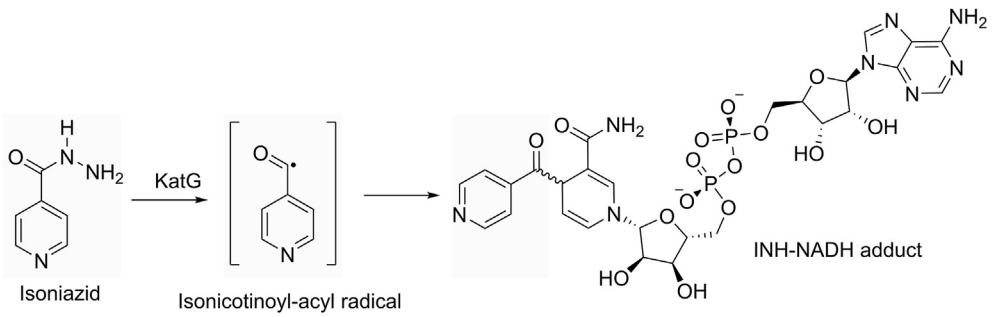

Scheme 1. Isoniazid activation by KatG enzyme.

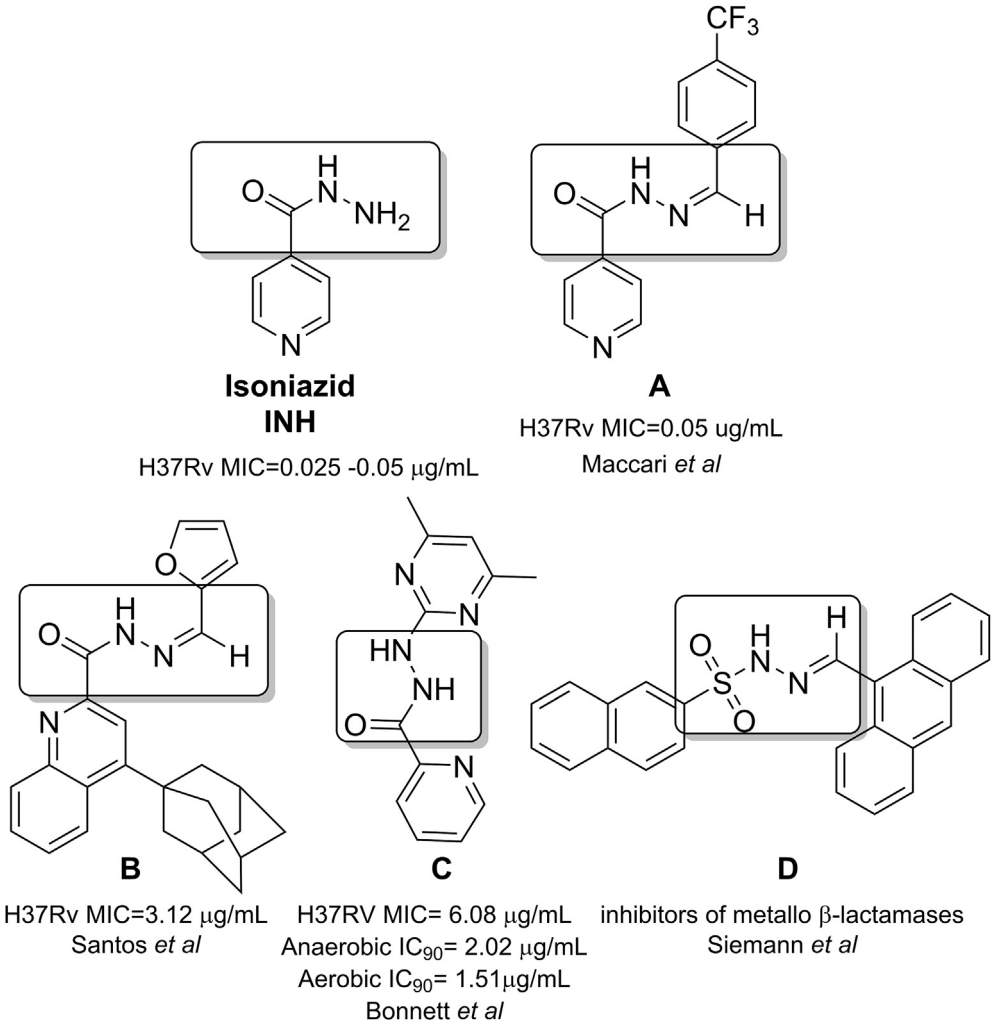

Fig. 1. Antitubercular INH related compounds.

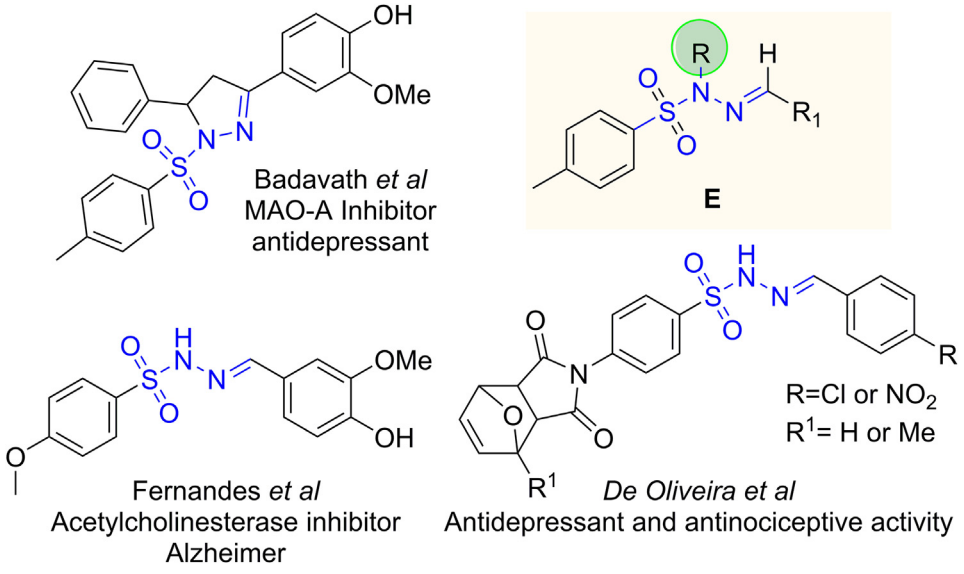

Fig. 2. Bioactive tosyl hydrazones.

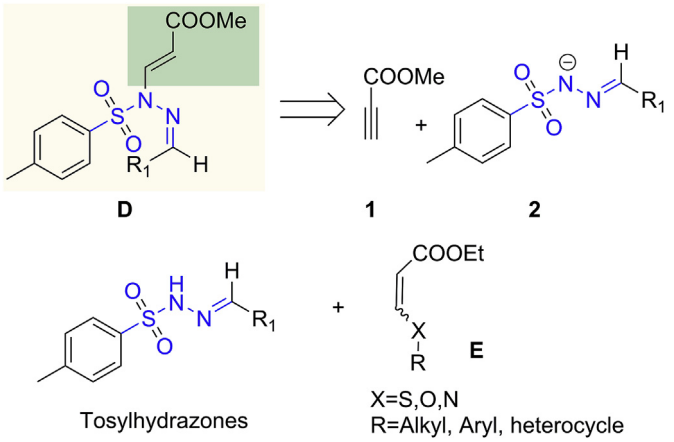

Scheme 2. Proposed merged scaffold and synthesis.

Hydrazones are known to be toxic and potentially explosive, being a major drawback when used in any synthetic scheme, particularly when being the starting material. That becomes particularly important for industrial applications where scaling up the synthesis is needed, handling grams to kilograms of diazo compounds [36]. That instability requires special care and convenient handling. As an alternative procedure to deal with those disadvantages, we have proposed a new alternative method involving a one-pot synthesis, without hydrazone intermediates isolation, to generate the acrylate derivates in a simple and safe manner. Therefore, it was necessary to find an alternative method that would allow us to prepare the hydrazone with a concomitant Michael reaction, without isolating the condensation product. Prof. Aggarwal's group has a long history of using diazo compounds as valuable synthetic intermediates [37]. Between those applications, they have reported a synthetic procedure to prepare pyrazoles. This reaction starts with the condensation of tosylhydrazine and benzaldehyde, followed by addition of an aqueous solution of sodium hydroxide. The benzaldehyde tosylhydrazone sodium salt **I**, formed the diazo intermediate **II** that reacts with an internal alkyne in a [3 + 2] cycloaddition (Route A, Scheme 3).

Our goal was to find conditions to capture the tosylhydrazone anion **I** with a Michael acceptor (Route B, Scheme 3) before spontaneously losing a sulfinate, generating the corresponding diazo intermediate. Thus, the aza-Michael reaction will be competing with a 1,3-dipolar cycloaddition. Previously, Kong et al. have studied this competing process in different conditions, analyzing the

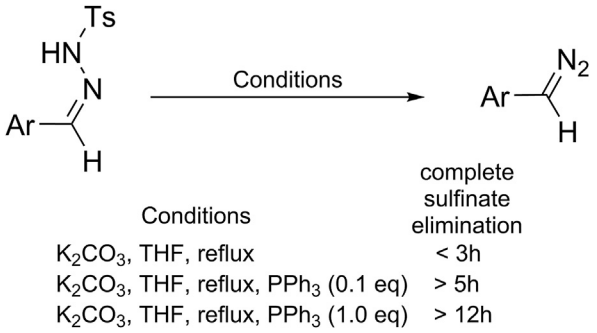

Scheme 4. Study of the stability of the tosylhidrazone anion by Kong et al.

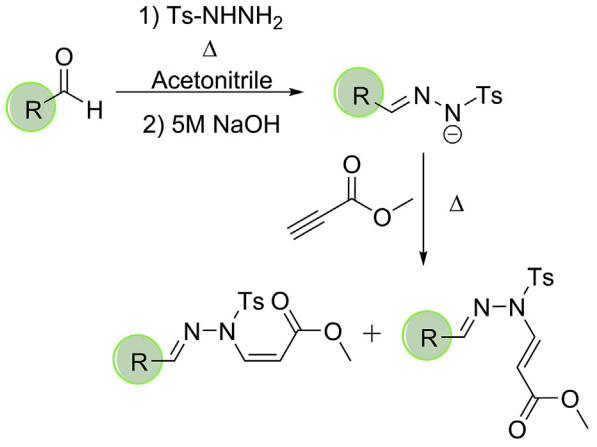

Scheme 5. Synthesis of tosylhydrazone acrylates.

effect of PPh_3 as a stabilizing agent of the tosylhydrazone anion [35] (Scheme 4). Without the addition of PPh_3, the tosylhydrazone anion decomposes in less than 3 h. Therefore, there is an open window of stability to add the Michael acceptor, that will afterwards react to produce the adduct (see Scheme 5).

We started the optimization process of the reaction using benzaldehyde as a model substrate. Initially, the hydrazone formation was attempted by the reaction of the aldehyde with tosylhydrazine in anhydrous acetonitrile at room temperature over several hours. To favor the formation of the reaction intermediate, it was necessary to run the reaction under reflux to promote the dehydration, adding molecular sieves to remove the water. Under

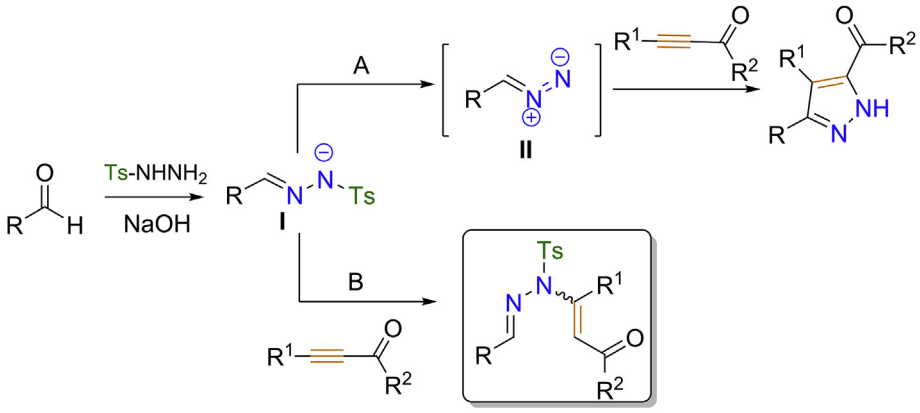

Scheme 3. Different possible pathway of the reaction.

that condition, it was possible to produce the intermediate, that was then treated with an aqueous solution of sodium hydroxide, leading to a solution of benzaldehyde tosylhydrazone sodium salt in 30 min. Finally, we proceeded to add methyl propionate and allow it to react overnight at room temperature. On our first attempts, only the *Z* isomer at low yields was obtained. To improve the yield, we decided to raise the temperature of this step, running the reaction at reflux. Under this condition the conversion was complete, obtaining a mixture of regioisomers in good yield and reducing the reaction time from 12 to 4 h.

Having optimized the reaction procedure, we studied the scope of the reaction with a diverse selection of aldehydes in order to prepare a collection of analogs. First, different substituted benzaldehydes were evaluated, generating derivatives **2** to **7** (Table 1) without substantial differences with the model substrate. 2-Naphthaldehyde was also used in order to have a higher steric demand; and the effects of a heteroatom on the aromatic ring was explored including furfural and pyrrole-2-carboxaldehyde. Reactions provided the expected products **8**, **9** and **10** with variable yields. Finally, the reactivity of α,β-unsaturated aldehydes was assayed obtaining the derivatives **11**–**15** in good yields. However, when pentaldehyde was used, no product was observed (Table 1).

All the isomers were successfully separated by flash column and characterized by ^{1}H and ^{13}C NMR, and mass spectrometry. The yields were calculated including both isolated isomers. The *E:Z* ratio was calculated by ^{1}H NMR signals and was near 40:60 for all the reactions. Following this methodology, it was possible to synthesize 30 compounds.

Table 1
N-Tosylacrylate synthesized.

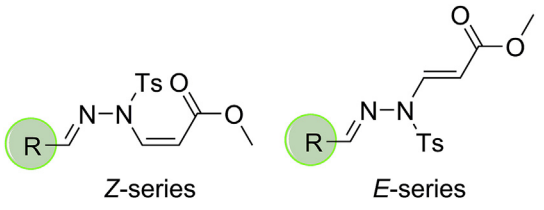

Substituent family	R	Compounds		Yield %
Aromatic	phenyl	**1E**	**1Z**	68
	2-OMe-Ph	**2E**	**2Z**	26
	2-CF_3-Ph	**3E**	**3Z**	58
	binaphtyl	**4E**	**4Z**	90
	4-NO_2-Ph	**5E**	**5Z**	50
	4-Br-Ph	**6E**	**6Z**	87
	3,4-diMeO -Ph	**7E**	**7Z**	67
	2-napthyl	**8E**	**8Z**	27
Heterocyclic		**9E**	**9Z**	71
		**10E**	**10Z**	42
α,β-unsaturated	prenyl	**11E**	**11Z**	52
		12E	**12Z**	33
		**13E**	**13Z**	85
		**14E**	**14Z**	35
	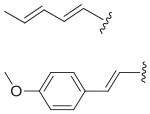	**15E**	**15Z**	63
Saturated	pentyl			Not observed

2.2. Biological evaluation

2.2.1. In vitro activity against M. tuberculosis

All of the synthesized N-acrylates were assayed in vitro against *M. tuberculosis* H37Rv obtaining the MIC by serial microdilution colorimetric assay using MTT as viability indicator [38,39]. The results are presented in Table 2 and Fig. 3. At the higher concentration tested (20 μM), seventeen of the analogs did not show antitubercular activity. The remaining thirteen derivatives (43% of the collection) showed MIC ranging from 20 to 1.25 μM. Of those, analogs **3E**, **8Z**, **10Z** and 1**4Z** had a MIC = 20 μM, three (**11Z**, **12E** and **15E)** displayed a MIC = 10 μM, and another three derivatives (**10E**, **11E** and **14E)** showed a MIC of 5.0 μM. Finally, the most active analogs were **1E**, **2E** and **8E** with MIC = 1.25 μM. The structure-activity relationship analysis indicates the importance of the regiochemistry of the acrylate on activity profile. Out of the thirteen active members of the collection, nine analogs were *E* isomers, and more importantly, were exclusively the compounds that displayed the best (below 10 μM) MIC.

A detailed analysis of the effect of the substituent shown evidence of steric and electronic effect have an impact on the activity profile of the compounds. The *E* isomer of the simplest aromatic derivative (**1E**) that holds a phenyl group was one of the most active compounds. The analogs with substituted phenyl rings shown that the *ortho* derivatives were more active than the *para* substituted ones. The substitution of the *para* position seems to be sensitive to the nature of the group. Activating substituent **2E** (**2-OMe**) conserved the potency display by the non-substituted derivative **1E**, meanwhile, a compound containing a strong deactivating methyltrifluoro group (**3E**), was inactive. The *para* substituted derivatives were all inactive, not being possible to infer any effect of activating and deactivating groups of the aromatic ring. On the other side, fused aromatic ring derivatives, like the naphthyl analog **8E,** were as active as analog **1E**, demonstrating that the size of the ring does not affect the potency when the regiochemistry is conserved**.** Only the furanyl analog **10** was active out of the two heterocyclic derivatives prepared. Derivatives **11** to **15** included different conjugated double bonds of different size and length. The activity of this series increases as the size of the substituent decreases, being derivatives **11E** and **14E** clear examples of that behavior.

Recently, Ghiya et al. have prepared and evaluated a library of N'-substituted-4-methylbenzenesulfonohydrazides for antimycobacterial, antibacterial and antifungal activities [40]. Those compounds were prepared from substituted benzaldehyde (Cl, Br, OMe) and p-toluensulphonyl hydrazine being similar to our proposed scaffold but lacking the N-methyl acrylates group. The

Table 2
Antimycobacterial activity compounds in MtH37Rv.

Compound	MIC μM	Compound	MIC μM	Compound	MIC μM
1Z	20	**6Z**	>20	**11Z**	10
1E	1.25	**6E**	>20	**11E**	5.0
2Z	>20	**7Z**	>20	**12Z**	>20
2E	1.25	**7E**	>20	**12E**	10
3Z	>20	**8Z**	20	**13Z**	>20
3E	20	**8E**	1.25	**13E**	>20
4Z	>20	**9Z**	>20	**14Z**	20
4E	>20	**9E**	>20	**14E**	5.0
5Z	>20	**10Z**	20	**15Z**	>20
5E	>20	**10E**	5.0	**15E**	10
INH	0.36	**Rif**	0.30		

INH = isoniazid Rif: Rifampycin

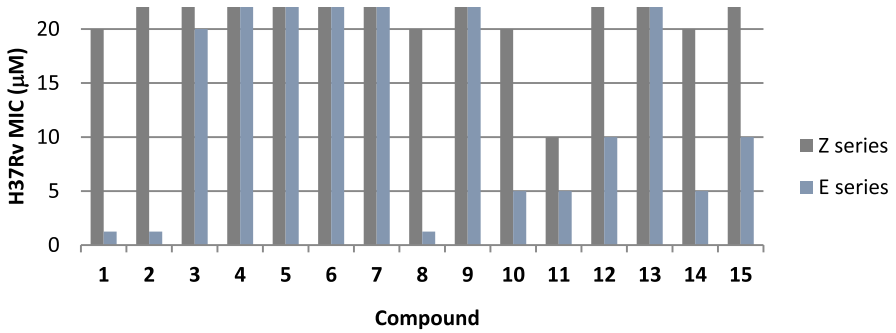

Fig. 3. Minimal Inhibitory Concentrations of the compounds prepared against *M. tuberculosis.*

activity of that library on *M. tuberculosis* H37Rv ranged from MIC = 411.1 μM−85.8 μM (for the 2,4-dimethoxy analog); that is four times less active than almost half of our library and 69 less active than compounds **1E**, **2E** and **8E,** the most active members of the collection. Therefore, the importance of the addition of a Michael acceptor on the structure is clearly relevant to improve the biological activity.

A comparison with the similar scaffold previously mentioned shown that the most active analogs **1E**, **2E** and **8E** are 6- and 20-fold more active than compounds **B** (MIC 7.8 μM) and **C** (MIC 25 μM) but did not reach the potency of INH and compound **A**. It is also important to compare the activity of those compounds with the parent drug INH. Analogs **1E**, **2E** and **8E** have a MIC that is 3.5 times higher than INH. Alternatively, we can also compare the activity of those analogs with rifampicin. This antimycobacterial polyketide is a key component of anti-tuberculosis therapy that targets the DNA-dependent RNA polymerase. The MIC of the aza-acrylates **1E**, **2E** and **8E** are 4.2 times higher than that of the antimycobacterial polyketide. That comparison suggest that further improvement is necessary on the proposed structures to reach rifampicin potency. Nevertheless, when compared to rifampicin, the aza-acrylates are synthetic small molecules that can be easily prepared, being excellent candidates for further development.

2.2.2. *In vitro cytotoxicity assay on Vero cells*

All the analogs were tested for cytotoxicity on VERO (monkey kidney fibroblast) cells by Neutral Red assay, lacking cytotoxicity up to the maximum concentration of 4.75 μg/mL. Taking into account this information, the most active compounds **1E, 2E** and **8E** have low cytotoxicity, with IC_{50} > 13.3 μM, > 12.2 μM and >11.6 μM, respectively. Those values correspond to selectivity index of 10.6, 9.76 and 9.28, which indicates that are good candidates to advance to *in vivo* studies [41].

2.2.3. *In vitro activity against MtInhA overexpressing strain*

Having in mind that the proposed scaffold was inspired by INH, we wanted to determine if our set of active compounds shared the same mechanism of action. To do that, we set to validate InhA as the main target of our compounds, towards that end we compared the activity of the most active compounds of our library on the wild-type H37Rv and on an InhA overexpressing *M. tuberculosis* strain (InhA-OE) [42]. In the former, an increase on the MIC will be suggestive of the role of this enzyme as an *in vivo* target as has been reported by several authors. For example, 4-hydroxy-2-pyridones have a ratio InhA-OE/H37Rv between 1.7 and 2.2 [43], meanwhile alkyl diphenyl ethers ranged between 9 and 12 [44,45], and thiadiazoles varied between 4-fold or more on *M. smegmatis* mc^2155 and *M. bovis* BCG strains expressing *M. tuberculosis* or *M. smegmatis* InhA [46]. As expected, the ratio is 20 times higher for INH and ethionamide respectively.

As it can be seen in Table 3 and Fig. 4**,** the MIC on the InhA-OE strain doubled the observed MIC for the wild type strain for the six compounds selected. Of note, the 2-fold difference was observed on a number of experimental repetitions. Those results indicate that InhA could be the target (or one of the targets) of these compounds.

To gain insight into the binding mode, the previously selected analogs (**1E**, **2E**, **8E**, **10E**, **11E** and **14E**) were docked on the crystallized enoyl-acyl carrier protein reductase protein (PDB ID 4TRO). The results showed that all the compounds had the same binding mode. They display a hydrogen bond interaction between the sulfonamide oxygen and Ile194 amide nitrogen that are at, on average, 2.15 Å and an average hydrogen bond angle of 159° (Fig. 5, Table 4). The distance between Tyr158 and the ester group is, on average, 1.78 Å and an average hydrogen bond angle of 152° (Fig. 5, Table 4), being another hydrogen bond interaction that contributes to the binding of the compounds.

This critical interaction of Tyr158 has also been found on the different crystal structures. Such an example is given by the crystal structure of InhA bound to a carbonyl arylamide inhibitor. In this structure, the oxygen of the amide carbonyl group is hydrogen-bonded to the hydroxyl group of Tyr158, very close to what was observed between the carbonyl group of the ester and the same residue [47]. Other examples included the alkyl diphenyl ethers, where the oxygen at the 4-hydroxy group of the inhibitor make hydrogen bond with the hydroxy group of the tyrosine [45], with 4-hydroxy-2-pyridone that displayed similar hydrogen-bonding pattern [43]. More recently, the crystal structure of diazaborines, a cofactor-independent class of inhibitors of enoyl fatty acyl reductases including InhA, showed hydrogen bonds and charge-charge interaction between the diazaborine head and Tyr158 [48].

Table 3
Compared activity against Mtb H37Rv and Mtb OE InhA.

Compound	MIC (μM)	
	H37Rv	InhA-OE
1E	1.25	2.5
2E	1.25	5.0
8E	1.25	2.5
10E	5.0	10
11E	5.0	10
14E	5.0	10
INH	0.36	>7.3

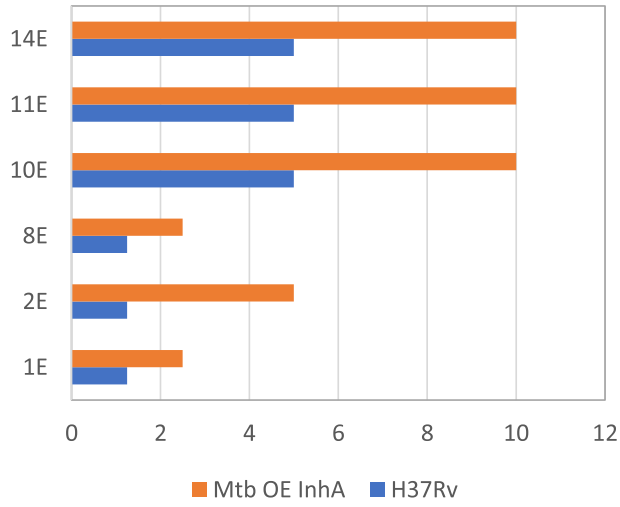

Fig. 4. Compared activity against Mtb H37Rv and Mtb OE InhA.

A detailed Autodock4 energy profile of the docking studies of the selected analogs is presented in Table 4. When the calculated score energy is compared with the MTb MIC, a similar tendency was observed. Nevertheless, comparison of the most active analogs displaying equal MIC values (1.25 μM) showed that the simplest analog **8E** seems to form the most stable complex, followed by **1E** and **2E**.

We can classify the compounds in two different groups when looking at hydrogen bond distances and angles to Ile194. 1E, 2E and 8E have tighter interactions (2.07 A and 157°) while 10E, 11E and 14E have higher H-bond distances (2.24 A and 160.5°). On the other hand, the H-bond distances and angles are quite similar between all the derivatives analyzed here.

The main difference in the observed activity could be explained by the type of hydrophobic R group. Aromatic interactions between aromatic R substituents and Phe97 could be involved in the observed better MIC and the computed Autodock4 Energy (Fig. 5, dashed lines). Nevertheless, we cannot discard that the change in hydrophobicity could also influence the ability of the compounds to penetrate the cell wall and thus, explain the different MIC between the compounds. The change in hydrophobicity can be seen in the computed clogP for the compounds (Table 4). The computed clogP of the compounds correlates quite well with the lipophilicity of them.

Table 4
MIC and Autodock4 Energy Score for receptor 4TRO with computed cLogP for each compound.

Compound	MIC μM	Autodock4 Energy (kcal/mol)	clogP
1E	1.25	−9.03	3.17
2E	1.25	−8.41	3.18
8E	1.25	−9.83	4.36
10E	5.00	−7.96	2.43
11E	5.00	−7.98	3.25
14E	5.00	−7.99	2.99

2.2.3.1. ADME-tox calculations and molecular properties calculations. An adequate balance between the partition coefficient and the solubility is necessary for oral drug good bioavailability. One-third of new chemical entities have poor pharmacokinetic properties and have not been able to reach the clinical trial phase. The experimentally expensive process to determine ADME-Tox properties of drug candidates can be accelerated by using *in silico* methods on early steps of the development pipeline. To that purpose, computational studies of all the synthesized compounds were performed to predict their physicochemical parameters, ADME properties, Lipinski's rule of five (Ro5), toxicity liabilities and drug-likeness. The rule of five proposed by Lipinski et al. [49] is a widely used filter which may indicate if a compound presents good theoretical oral bioavailability (logP, MW, nON, and nNHOH). Veber expanded with other parameters (ROT and PSA) that contribute to a better prediction of oral absorption and bioavailability [50].

Because the analysis cannot differentiate between *E* and *Z* regioisomers, only 15 calculations were necessary. To complete the analyses, the data were compared with first-line drugs used for TB treatment (isoniazid—INH—, rifampicin-RIF-, pyrazinamide-PZA-, ethambutol-EMB- and streptomycin-SM-).

The results presented in Table 5 show that all the compounds have MW < 500, log P < 5 and the number of hydrogen bond acceptors and donors also fulfill the Ro5. The prepared compounds also obey Veber parameters [50]. In summary, all the compounds that form the collection seem to be good candidates in term of satisfactory membrane permeability and oral bioavailability and, thus, might be considered as drug-like molecules. As was expected, two of the first-line drugs (rifampicin and streptomycin), violate some of the rules, demonstrating that Ro5 may not be considered strictly [51].

The Osiris platform [52] predicted the overall toxicity based on the presence of fragments responsible for irritant, mutagenic, tumorigenic, or reproductive effects. The calculations shown in Table 6 revealed that all compounds, except for compound **5,** present a low toxicity risk. When compared to the first line drug INH, it

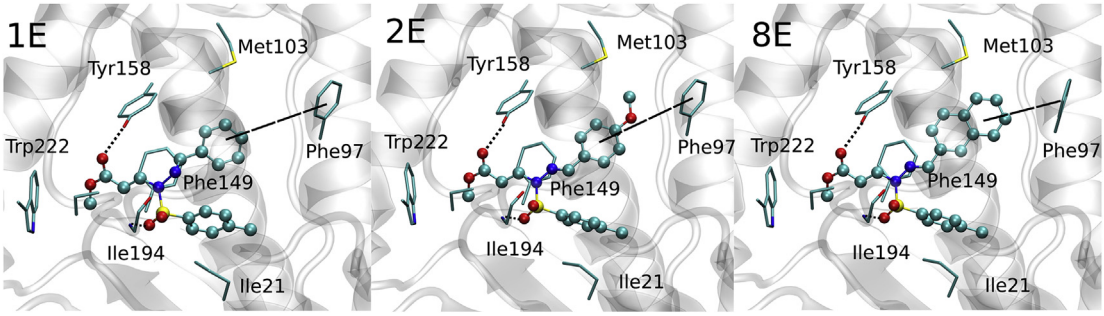

Fig. 5. Docking poses of analogs **1E**, **2E**, **8E** on InhA PDB ID 4TRO. Protein backbone is depicted in New cartoon representation in transparent background. Key residues are shown as sticks while compounds are shown with Ball and Sticks representation. Color code of atoms: Carbon (Cyan), Nitrogen (Blue), Oxygen (Red) and Sulphur (Yellow). Point lines depict Hydrogen Bonds while dashed lines indicate Pi-Pi interaction between aromatic centers. (For interpretation of the references to color in this figure legend, the reader is referred to the Web version of this article.)

Table 5
In silico parameters of acrylates compounds and first-line drugs.

Compound	MW	logP	n ON	nNHOH	TPSA	ROT	Viol.
1–15	347–436	0.91–3.79		0–1	84.42–144.1	7–9	0
INH	137	−0.97	4	3	68.01	1	0
EMB	204	0.35	4	4	64.51	9	0
RIF	822	2.10	16	6	216.6	5	3
SM	581	−7.86	19	16	336.4	11	3
PZA	123	−0.71	4	2	68.88	1	0
Lipinski [49]	<500	≤5	<5	<10			
Veber [50]					≤140	≤10	

Table 6
In silico toxicity risks and drugs-score of acrylates compounds and first line drugs.

Compound	Toxicity risks[a]				Drug-score	
	M[b]	T[c]	I[d]	Re[e]	Drug likeness	Drug-score
1–15	-	-	-	-	−16.4 to −4.23	0.14–0.45
INH	+	+	+	+	−5.06	0.06
EMB	-	-	+	-	2.38	0.56
RIF	-	-	-	+	10.12	0.2
SM	-	-	+	-	0.83	0.32
PZA	+	+	-	+	−0.68	0.14

[a] Ranked according to: (−) not toxic, (±) slightly toxic, (+) highly toxic.
[b] M, mutagenic;
[c] T, tumorigenic;
[d] I, irritant;
[e] Re, reproductive effective.

has high toxicity risks for all the indicators, and the other five drugs presented at least one alert.

Comparing the drug-likeness of the compounds against first-line drugs, positive drug-likeness value (0.1–10) points out that a molecule contains predominantly fragments which are frequently present in commercial drugs; we found lower values of drug-likeness for the compounds with the exception analog 7 which is better than isoniazid.

The drug-score combines drug-likeness, lipophilicity, solubility, molecular weight, and toxicity risks all in one value, and this may be used to judge the compound overall potential as a drug. As seen from results collected in Table 7, the most active compounds showed low to moderate drug-score (0.14–0.45) that revealed their potential as safe lead compounds. Most of the compounds have higher values than first-line drugs except for ethambutol.

A rapid comparison between the most active compounds of the series against INH (Table 7) shows a clear contrast. While the aza-acrylates do not have toxicity risks, INH showed high toxicity risks as observed in patients under treatment with INH. The logP values of the compounds are in the accepted range, while the negative value for INH confirms the low solubility in water. PSA values suggest that both the new compounds as well as INH have good permeability of biological membranes. Because drug-score calculations are performed considering the toxicity and physical properties, the drug-score is about 5 times higher in our series than the calculated for INH. The lowest MIC obtained in our series is 4 times higher than that of INH. However, the drug-score value and low toxicity point out that these NCE are interesting candidates for antimycobacterial drug development.

As InhA is an important target for new antimycobacterial drug development, a wide range of inhibitors has been previously reported. A search on the ChEMBL database, a chemical database of bioactive molecules maintained by the European Bioinformatics Institute (EMBL-EBI) [53], provided 322 compounds with reported activity on the enzyme. In Fig. 6 we can observe that the physico-chemical parameters (logP, MW and TPSA) of the most active compounds of the library shown in Table 7 are in the same range of the wide collection of InhA inhibitors reported.

To define the explored chemical space between the reported InhA inhibitors (the 322 InhA inhibitors found on ChEMBL) and our collection, a similarity search was performed using the web-based platform chemmine tools [54] using a *Tanimoto coefficient*> 0.7. The results were plotted in a three-dimensional space group according to the different clusters found. The 30 synthesized analogs were also included in the same analysis to identify their similarity with the reported inhibitors. Fig. 7 shows the different clusters found, where the aza-acrylate are grouped (orange) in a different cluster. The analysis performed demonstrates that the prepared collection has low similarity with previously reported compounds and is a new chemotype that is located in an unexplored section of the chemical space of the InhA inhibitors.

3. Conclusions

In summary, we have prepared fifteen *E,Z* pairs of N-substituted tosyl N'-acryl hydrazine acrylates with good yields. This collection was assayed against *M. tuberculosis*, nine of then having a MIC of 10 μM or below. The most active compounds **1E**, **2E** and **8E** are *E* isomers holding bulky aromatic (phenyl and naphthyl) substituents. As pointed out, the acrylate group is critical for the antimycobacterial activity, identifying a potent novel scaffold (Fig. 8). We have tested the compounds against an InhA over-expressing strain, obtaining MIC differences suggesting that the compounds could potentially inhibit the enzyme. Docking studies, performed to rationalize how the compounds interact with the enzyme, found that hydrogen bond interactions with Tyr 158 and

Table 7
In silico parameters and biological activities of acrylates *hits* and INH.

Compd	Toxicity risks	MW	logP	PSA	Drug-score	MIC[a] μM	CYT[b] μM	SI[c]
1E	- - - -	358	3.17	76.05	0.43	1.25	>13.3	10.6
2E	- - - -	388	3.18	85.28	0.41	1.25	>12.2	9.76
8E	- - - -	408	4.36	76.05	0.33	1.25	>11.6	9.28
INH	++++	137	−1.02	68.01	0.06	0.37		

[a] Activity against Mtb HR37Rv.
[b] Citotoxicity against Vero cells.
[c] Selectivity index.

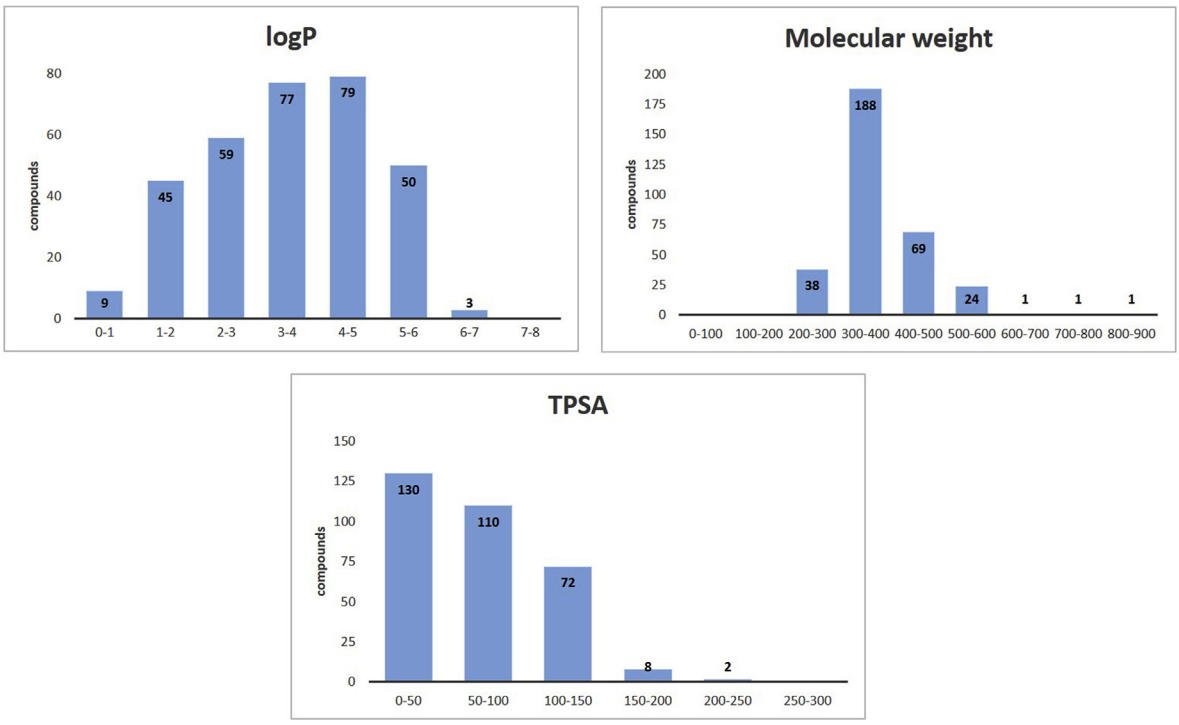

Fig. 6. Distribution of physicochemical parameters of the chemical library.

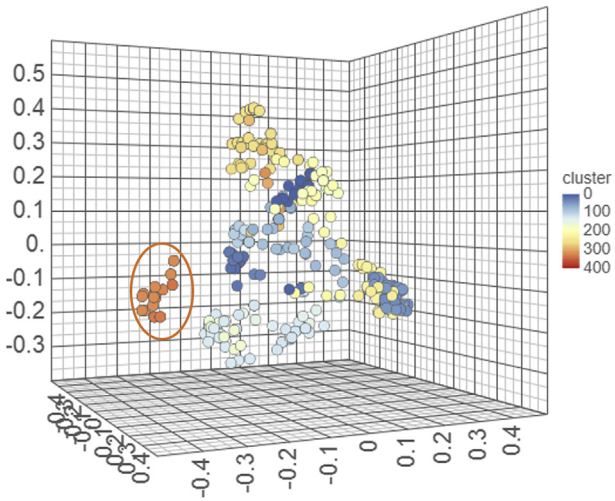

Fig. 7. Analysis of molecular similarity of known InhA inhibitors and the prepared collection (highlighted in orange). (For interpretation of the references to color in this figure legend, the reader is referred to the Web version of this article.)

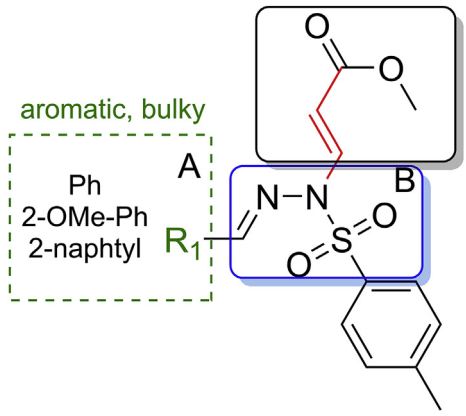

Fig. 8. SAR analysis of the aza acrylates chemical library.

Ile194 were critical for binding InhA, in agreement with results by Parikh [55,56] and Khan [57]. A complete chemoinformatics analysis of the collection was also performed, suggesting that the compounds have no toxicity risk and comply with Lipinski's Ro5. A similarity search of the prepared collection with known InhA inhibitors revealed that the new INH inspired analogs are located in an unexplored region of the chemical space. Isolation and characterization of *M. tuberculosis* mutants resistant to compounds **1E**, **2E** and **8E** will shed light on whether they bind InhA and help understanding the protein-compound molecular interactions *in vivo*. Thus, we consider that the aza-acrylate is a promising scaffold for antitubercular drug discovery that prompt further studies on their mechanism of action to completely validate InhA as the main molecular target.

4. Material and methods

4.1. General

All reactions were performed under nitrogen atmosphere using oven-dried glassware and standard syringe/septa techniques. The reaction progress was monitored on GP TLC plates. Spots were visualized under 254 nm UV light and/or by dipping the TLC plate into a solution of 2 mL anisaldehyde and 10 mL glacial acetic acid and followed by heating with a heat gun. Column chromatography was performed with silica gel 60 (230–400 mesh) under a low pressure of nitrogen, using increasing EtOAc-hexane gradients as a solvent. All the solvents (hexane, ethyl acetate, acetonitrile) were distilled before use.

^{1}H and ^{13}C NMR spectra were measured on a 300 MHz Bruker Avance II using $CDCl_3$ as a solvent. Chemical shifts were reported in ppm downfield from tetramethylsilane (δ) as the internal standards and coupling constants are in hertz (Hz). Assignments of proton resonances were confirmed by correlated spectroscopy (Heteronuclear Single Quantum Coherence, HSQC) high-resolution mass spectra (HRMS) were recorded on a Bruker MicroTOF II spray source. All the melting points were determined in open Pyrex capillaries with an Electrothermal 9000 melting point apparatus and are uncorrected.

4.2. Synthesis

4.2.1. General procedure for the preparation of acrylates

The p-toluene sulfonyl hydrazide (279 mg, 1.5 mmol) was added to a solution of aldehyde (1.5 mmol) in dry acetonitrile and the mixture was stirred at 90 °C for 6 h. A solution of 5 M NaOH (1.5 mmol) was added and the mixture was stirred for another 30 min at RT. Then the propiolate (7.5 mmol) was added dropwise, and the mixture was stirred at 90 °C. The volatiles were evaporated under reduced pressure, and the residue was dissolved in a 1:1 mixture of brine-ethylacetate (70 mL). The organic layer was separated and dried over Na_2SO_4. After filtration and removal of the solvent under reduced pressure, the crude material was purified by flash chromatography over silica gel using an increasing AcOEt/hexane gradient.

*4.2.1.1. Methyl (Z)-3-(2-((E)-benzylidene)-1-tosylhydrazinyl) acrylate (**1Z**).* Colourless oil. ^{1}H NMR (300 MHz, $CDCl_3$): δ 8.24 (s, 1H, C4−H), 7.74 (d, J = 8.3 Hz, 2H, H_{arom}), 7.65 (d, J = 8.1, 2H, C5−H), 7.43-7.40 (m, 3H, H_{arom}), 7.31 (d, J = 8.1 Hz, 2H, C6−H), 6.53 (d, J = 9.1 Hz, 1H, C3−H), 5.65 (d, J = 9.1 Hz, 1H, C2−H), 3.57 (s, 3H, OCH_3), 2.42 (s, 3H, Ts-CH_3). ^{13}C NMR (75 MHz $CDCl_3$): δ 165.5 (CH), 158.3 (C), 144.9 (C), 134.2 (CH), 133.3 (C), 133.1 (CH), 131.5 (C), 130.0 (CH), 129.7 (CH), 128.8 (CH), 128.3 (CH), 113.3 (CH), 51.7 (CH_3), 21.6 (CH_3). IR (film) υ: 3061, 1712, 1625, 1604, 1435, 1170, 1143, 1087, 813, 704, 657, 574 cm^{-1}. ESI-HRMS Calcd for (M + H$^+$) $C_{18}H_{19}N_2O_4S$ 359.1060, found 359.1060.

*4.2.1.2. Methyl (E)-3-(2-((E)-benzylidene)-1-tosylhydrazinyl) acrylate **(1E)**.* Colourless oil. ^{1}H NMR (300 MHz, $CDCl_3$): δ 8.69 (s, 1H, C4−H), 8.12 (d, J = 13.6 Hz, 1H, C3−H), 7.77 (d, J = 7.5 Hz, 2H, H_{arom}), 7.65 (d, J = 8.5 Hz, 2H, C5−H), 7.53 (d, J = 7.3 Hz, 1H, H_{arom}), 7.46 (d, J = 7.5 Hz, 2H, H_{arom}), 7.31 (d, J = 8.2 Hz, 2H, C6−H), 5.37 (d, J = 13.6 Hz, 1H, C2−H), 3.70 (s, 3H, OCH_3), 2.43 (s, 3H, $TsCH_3$). ^{13}C NMR (75 MHz, $CDCl_3$): δ 169.4 (CH), 167.3 (C), 145.3 (C), 141.8 (CH), 133.7 (C), 132.8 (CH), 132.3 (C), 129.9 (CH), 129.1 (CH), 129.0 (CH), 127.9 (CH), 102.0 (CH), 51.4 (CH_3), 21.7 (CH_3). IR (film) υ: 3061, 1712, 1625, 1604, 1435, 1170, 1143, 1087, 813, 704, 657, 574 cm^{-1}. ESI-HRMS Calcd for (M + H$^+$) $C_{18}H_{19}N_2O_4S$ 359.1060, found 359.1060.

*4.2.1.3. Methyl (Z)-3-(2-((E)-2-methoxybenzylidene)-1-tosylhydrazinyl) acrylate (**2Z**).* Colorless oil. ^{1}H NMR (300 MHz, $CDCl_3$): δ 8.59 (s, 1H, C4−H), 7.73 (m, 3H, H_{arom}-C5-H), 7.39 (m, 1H, H_{arom}), 7.29 (d, J = 8.1 Hz, 2H, C6−H), 6.95 (d, J = 7.6 Hz, 1H, H_{arom}), 6.89 (d, J = 7.9 Hz, 1H, H_{arom}), 6.46 (d, J = 9.2 Hz, 1H, C3−H), 5.65 (d, J = 9.2 Hz, 1H, C2−H), 3.85 (s, 3H, OCH_3), 3.60 (s, 3H, OCH_3), 2.41 (s, 3H, Ts-CH_3). ^{13}C NMR (75 MHz, $CDCl_3$): δ 165.6 (C), 158.8 (C), 153.6 (CH), 144.7 (C), 134.4 (C), 133.4 (CH), 132.8 (CH), 129.6 (CH), 128.3 (CH); 126.8 (CH), 121.6 (C), 120.7 (CH), 113.5 (CH), 111.1 (CH), 55.6 (CH_3), 51.6 (CH_3), 21.6 (CH_3). IR (film) υ: 1714, 1624, 1597, 1487, 1436, 1371, 1288, 1253, 1170, 1145, 1087, 1045, 756, 705, 659 cm^{-1}. ESI-HRMS Calcd for (M + H$^+$) $C_{19}H_{21}N_2O_5S$ 389.1166, found 389.1166.

*4.2.1.4. Methyl (E)-3-(2-((E)-2-methoxybenzylidene)-1-tosylhydrazinyl) acrylate (**2E**).* White solid. Mp: 154.8−155.8 °C. ^{1}H NMR (300 MHz, $CDCl_3$): δ 9.08 (s, 1H, C4−H), 8.12 (d, J = 13.5 Hz, 1H, C3−H), 7.90 (d, J = 7.5 Hz, 1H, H_{arom}), 7.67 (d, J = 8.6 Hz, 2H, C5−H), 7.50 (d, J = 8.2 Hz, 1H, H_{arom}), 7.32 (d, J = 7.9 Hz, 2H, C6−H), 6.97 (t, J = 8.0 Hz, 2H, H_{arom}), 5.32 (d, J = 13.5 Hz, 1H, C2−H), 3.89 (s, 3H, OCH_3), 3.69 (s, 3H, OCH_3), 2.43 (s, 3H, Ts-CH_3). ^{13}C NMR (75 MHz, $CDCl_3$): δ 167.4 (C), 166.1 (CH), 159.6 (C), 145.1 (C), 141.9 (CH), 134.4 (CH), 133.8 (C), 129.9 (CH), 128.0 (CH), 127.4 (CH), 120.8 (CH), 111.3 (CH), 101.5 (CH), 55.7 (CH_3), 51.4 (CH_3), 21.7 (CH_3). IR (KBr) υ: 1714, 1624, 1597, 1487, 1436, 1371, 1288, 1253, 1170, 1145, 1087, 1045, 756, 705, 659 cm^{-1}.ESI-HRMS Calcd for (M + H$^+$) $C_{19}H_{21}N_2O_5S$ 389.1166, found 389.1166.

*4.2.1.5. Methyl (Z)-3-(1-tosyl-2-((E)-2-(trifluoromethyl)benzylidene) hydrazinyl) acrylate (**3Z**).* Colorless oil. ^{1}H NMR(300 MHz, $CDCl_3$): δ 8.23 (s, 1H, C4−H), 8.07 (d, J = 7.8 Hz, 1H, H_{arom}), 7.81 (d, J = 8.4 Hz, 2H, C5−H), 7.67 (d, J = 7.8 Hz, 1H, H_{arom}), 7.57- 7.49 (m, 2H, H_{arom}), 7.32 (d, J = 8.0 Hz, 2H, C6−H), 6.39 (d, J = 8.8 Hz, 1H, C3−H), 5.91 (d, J = 8.8 Hz, 1H, C2−H), 3.66 (s, 3H, OCH_3), 2.42 (s, 3H, Ts-CH_3).^{13}C NMR (75 MHz, $CDCl_3$): δ 164.8 (C), 146.8 (CH), 145.0 (C), 134.2 (C), 132.1 (CHx2), 131.3 (CH); 130.3 (CH), 129.8 (CH), 128.3 (CH), 127.5 (CH), 125.9 (CH), 117.8 (CH), 51.8 (CH_3), 21.6 (CH_3). IR (film) υ: 1714, 1624, 1597, 1438, 1315, 1166, 1122, 1033, 769, 671 cm^{-1}. ESI-HRMS Calcd for (M + H$^+$) $C_{19}H_{17}N_2NaO_4S$ 449.0753, found 449.0753.

*4.2.1.6. Methyl (E)-3-(1-tosyl-2-((E)-2-(trifluoromethyl)benzylidene) hydrazinyl) acrylate (**3E**).* Colorless oil. ^{1}H NMR (300 MHz, $CDCl_3$): δ 9.05 (s, 1H, C4−H), 8.17 (d, J = 13.5 Hz, 1H, C3−H), 8.14-8.11 (m, 1H, H_{arom}), 7.80-7.74 (m, 1H, H_{arom}), 7.69 (d, J = 13.5 Hz, 2H, C5−H), 7.62-7.58 (m, 2H, H_{arom}), 7.32 (d, J = 8.1 Hz, 2H, C6−H), 5.52 (d, J = 13.5 Hz, 1H, C2−H), 3.73 (s, 3H, OCH_3), 2.42 (s, 3H, Ts-CH_3). ^{13}C NMR (75 MHz, $CDCl_3$): δ 167.2 (C), 160.1 (CH), 145.7 (C), 143.7 (C), 141.4 (CH), 133.6 (C), 132.2 (CHx2), 131.7 (C), 130.1 (CH), 128.4 (C), 128.1 (CH), 127.9 (CH), 126.2 (CH), 102.4 (CH), 51.5 (CH_3), 21.7 (CH_3). IR (film) υ: 1714, 1624, 1597, 1438, 1315, 1166, 1122, 1033, 769, 671 cm^{-1}.ESI-HRMS Calcd for (M + H$^+$) $C_{19}H_{17}N_2NaO_4S$ 449.0753, found 449.0753.

*4.2.1.7. Methyl (Z)-3-(2-((E)-[1,1′-biphenyl]-4-ylmethylene)-1-tosylhydrazinyl) acrylate (**4Z**).* Colourless oil. ^{1}H NMR (300 MHz, $CDCl_3$): δ 8.30 (s, 1H, C4−H), 7.76-7.72 (m, 4H, H_{arom}), 7.65-7.60 (m, 4H, H_{arom}), 7.49-7.43 (m, 2H, H_{arom}), 7.40-7.38 (m, 1H, H_{arom}), 7.31 (d, J = 8.1 Hz, 2H, C6−H), 6.57 (d, J = 9.2 Hz, 1H, C3−H), 5.65 (d, J = 9.2 Hz, 1H, C2−H), 3.59 (s, 3H, OCH_3), 2.42 (s, 3H, Ts-CH_3). ^{13}C NMR (75 MHz, $CDCl_3$): δ 165.5 (C), 158.4 (CH), 144.9 (C), 144.2 (C), 140.0 (C), 134.2 (C), 133.4 (CH), 132.0 (C), 129.7 (CH), 129.0 (CH), 128.9 (CH), 128.7 (CH), 128.3 (CH), 127.5 (CH), 127.1 (CH), 112.8 (CH), 51.7 (CH_3), 21.7 (CH_3). IR (film) υ: 3062, 3030, 2993, 2951, 2920, 2848, 1714, 1623, 1600, 1371, 1170, 1145, 1087 cm^{-1}. ESI-HRMS Calcd for (M + H$^+$) $C_{24}H_{22}N_2NaO_4S$ 457.1192, found 457.1193.

*4.2.1.8. Methyl (E)-3-(2-((E)-[1,1′-biphenyl]-4-ylmethylene)-1-tosylhydrazinyl)acrylate (**4E**).* White solid. Mp 107−109 °C.NMR (300 MHz, $CDCl_3$): δ 8.73 (s, 1H, C4−H), 8.13 (d, J = 13.5, 1H, C3−H), 7.85 (d, J = 8.31, 2H, H_{arom}), 7.72-7.60 (m, 6H, H_{arom}-C5-H), 7.48 (t, J = 7.3 Hz, 2H), 7.42 (d, J = 7.1 Hz, 1H), 7.33 (d, J = 8.1, 2H, C6−H), 5.39 (d, J = 13.5 Hz, 1H, C2−H), 3.71 (s, 3H, OCH_3), 2.44 (s, 3H, Ts-CH_3). ^{13}C NMR (75 MHz, $CDCl_3$): 169.0 (CH), 167.3 (C), 145.6 (C), 145.3(C), 141.8 (CH), 139.8 (C), 133.7 (C), 131.1(C), 130.0 (CH), 129.6 (CH), 129.0 (CH), 128.3 (CH), 128.0 (CH), 127.6 (CH), 127.2 (CH), 101.9 (CH), 51.42 (CH_3), 21.7 (CH_3).IR (KBr) υ: 3062, 3030, 2993, 2951, 2920, 2848, 1714, 1623, 1600, 1371, 1170, 1145, 1087 cm^{-1}. ESI-HRMS Calcd for (M + H$^+$) $C_{24}H_{22}N_2NaO_4S$ 457.1192, found 457.1193.

*4.2.1.9. Methyl (Z)-3-(2-((E)-4-nitrobenzylidene)-1-tosylhydrazinyl) acrylate (**5Z**).* White solid. Mp: 120.0–121.0 °C. ^{1}H NMR (300 MHz, $CDCl_3$): δ 8.24 (d, *J* = 8.9 Hz, 2H, H_{arom}), 7.98 (s, 1H, C4–H), 7.78 (t, *J* = 8.2 Hz, 4H, H_{arom}-C5-H), 7.33 (d, *J* = 8.0 Hz, 2H, C6–H), 6.37 (d, *J* = 8.7 Hz, 1H, C3–H), 5.93 (d, *J* = 8.7 Hz, 1H, C2–H), 3.68 (s, 3H, OCH_3), 2.42 (s, 3H, Ts-CH_3). ^{13}C NMR (75 MHz, $CDCl_3$): δ 164.7 (C), 148.9 (CH), 148.7 (C), 145.3 (C), 139.1 (C), 134.1(C), 132.1 (CH), 129.8 (CH), 128.4 (CH), 128.3 (CH), 124.1 (CH), 118.2 (CH), 51.9 (CH_3), 21.7 (CH_3). IR (KBr) υ: 1732, 1597, 1519, 1435, 1344, 1172, 1087, 1037, 854, 748, 671 cm^{-1}. ESI-HRMS Calcd for (M + H^+) $C_{18}H_{17}N_3NaO_6S$ 426.0730, found 426.0730.

*4.2.1.10. Methyl (E)-3-(2-((E)-4-nitrobenzylidene)-1-tosylhydrazinyl) acrylate (**5E**).* Colourless oil. ^{1}H NMR (300 MHz, $CDCl_3$): δ 8.78 (s, 1H, C4–H), 8.29 (d, *J* = 8.6 Hz, 2H, H_{arom}), 8.10 (d, *J* = 13.5 Hz, 1H, C3–H), 7.92 (d, *J* = 8.6 Hz, 2H, H_{arom}), 7.66 (d, *J* = 8.3 Hz, 2H, C5–H), 7.33 (d, *J* = 8.6 Hz, 2H, C6–H), 5.54 (d, *J* = 13.5 Hz, 1H, C2–H), 3.74 (s, 3H, OCH_3), 2.74 (s, 3H, Ts-CH_3). ^{13}C NMR (75 MHz, $CDCl_3$): δ 167.0 (C), 162.0 (CH), 145.9 (C), 141.2 (CH), 138.1 (C), 133.4 (C), 130.2 (CH), 129.5 (CH), 127.8 (CH), 124.2 (CH), 103.2 (CH), 51.6 (CH_3), 21.7 (CH_3).IR (film)ν: 1732, 1597, 1519, 1435, 1344, 1172, 1087, 1037, 854, 748, 671 cm^{-1}. ESI-HRMS Calcd for (M + H^+) $C_{18}H_{17}N_3NaO_6S$ 426.0730, found 426.0730.

*4.2.1.11. Methyl (Z)-3-(2-((E)-4-bromobenzylidene)-1-tosylhydrazinyl) acrylate (**6Z**).* White solid. Mp: 120.2–121.0 °C. ^{1}H NMR (300 MHz, $CDCl_3$): δ 8.11 (s, 1H, C4–H), 7.72 (d, *J* = 8.2 Hz, 2H, C5–H), 7.51 (m, 4H, H_{arom}), 7.30 (d, *J* = 8.2, 2H, C6–H), 6.48 (d, *J* = 8.3 Hz, 1H, C3–H), 5.69 (d, *J* = 9.0 Hz, 1H, C2–H), 3.59 (s, 3H, OCH_3), 2.41 (s, 3H, Ts-CH_3). ^{13}C NMR (75 MHz, $CDCl_3$): δ 165.3 (C), 155.6 (CH), 145.0 (C), 134.1 (C), 133.1 (CH), 132.1 (CH), 129.8 (CH), 129.4 (CH), 128.2 (CH), 125.9 (C), 114.2 (CH), 51.7 (CH_3), 21.6 (CH_3). IR (KBr) ν: 1730, 1643, 1591, 1487, 1435, 1359, 1280, 1172, 1087, 1068, 1008, 817, 738, 667 cm^{-1}. ESI-HRMS Calcd for (M + H^+) $C_{18}H_{18}BrN_2O_4S$ 437.0165, found 437.0165.

*4.2.1.12. Methyl (E)-3-(2-((E)-4-bromobenzylidene)-1-tosylhydrazinyl) acrylate (**6E**).* Colourless oil. ^{1}H NMR(300 MHz, $CDCl_3$): δ 8.65 (s, 1H, C4–H), 8.10 (d, *J* = 13.4 Hz, 1H, C3–H), 7.65-7.61 (m, 6H, H_{arom}-C5-H), 7.31 (d, *J* = 8.0 Hz, 2H, C6–H), 5.37 (d, *J* = 13.4 Hz, 1H, C2–H), 3.71 (s, 3H, OCH_3), 2.43 (s, 3H, Ts-CH_3). ^{13}C NMR (75 MHz, $CDCl_3$): δ 167.3 (CH), 167.2 (C), 145.4 (C), 141.6 (CH), 133.6 (C), 132.4 (C), 131.2 (CH), 130.3 (CH), 130.0 (CH), 127.9 (CH), 127.6 (C), 102.2 (CH), 51.5 (CH_3), 21.7 (CH_3). IR (film)ν: 1730, 1643, 1591, 1487, 1435, 1359, 1280, 1172, 1087, 1068, 1008, 817, 738, 667 cm^{-1}. ESI-HRMS Calcd for (M + H^+) $C_{18}H_{18}BrN_2O_4S$ 437.0165, found 437.0165.

*4.2.1.13. Methyl (Z)-3-(2-((E)-3,4-dimethoxybenzylidene)-1-tosylhydrazinyl) acrylate (**7Z**).* Colourless oil. ^{1}H NMR (300 MHz, $CDCl_3$): δ 8.34 (s, 1H, C4–H), 7.85 (d, *J* = 8.2 Hz, 1H, H_{arom}), 7.70 (d, *J* = 8.3 Hz, 2H, C5–H), 7.29 (d, *J* = 8.0 Hz, 2H, C6–H), 7.19 (m, 1H, H_{arom}), 6.88 (d, *J* = 8.2 Hz, 1H, H_{arom}), 6.67 (d, *J* = 9.3 Hz, 1H, C3–H), 5.48 (d, *J* = 9.3 Hz, 1H, C2–H), 3.92 (s, 3H, OCH_3), 3.89 (s, 3H, OCH_3), 3.51 (s, 3H, OCH_3), 2.42 (s, 3H, Ts-CH_3). ^{13}C NMR (75 MHz, $CDCl_3$): δ 170.2 (CH), 166.2 (C), 154.5 (C), 153.4 (C), 141.9 (CH), 134.2 (C), 129.9 (CH), 128.0 (CHx2), 126.9 (C), 125.4 (C), 110.4 (CH), 109.0 (CH), 101.5 (CH), 56.0 (CH_3x2), 51.4 (CH_3), 21.7 (CH_3). IR (film)ν: 1730, 1597, 1514, 1438, 1267, 1166, 1024, 813, 765 cm^{-1}. ESI-HRMS Calcd for (M + H^+) $C_{20}H_{22}N_2NaO_4S$ 441.1091, found 441.1091.

*4.2.1.14. Methyl (E)-3-(2-((E)-3,4-dimethoxybenzylidene)-1-tosylhydrazinyl) acrylate (**7E**).* Colourless oil. ^{1}H NMR (300 MHz, $CDCl_3$) δ 8.56 (s, 1H, C4–H), 8.11 (d, *J* = 13.5 Hz, 1H, C3–H), 7.64 (d, *J* = 8.1 Hz, 2H, C5–H), 7.34- 7.28 (m, 4H, H_{arom}-C6-H), 6.90 (d, *J* = 8.3 Hz, 1H, H_{arom}), 5.31 (d, *J* = 13.5 Hz, 1H, C2–H), 3.93 (s, 3H, OCH_3), 3.88 (s, 3H, OCH_3), 3.67 (s, 3H, OCH_3), 2.40 (s, 3H, $TsCH_3$). ^{13}C NMR (75 MHz, $CDCl_3$): δ 170.2 (CH), 167.3 (C), 153.4 (C), 149.5 (C), 145.2 (C), 141.9 (CH), 133.8 (C), 129.9 (CH), 128.0 (CH), 125.4 (CH), 125.0 (C), 110.7 (CH), 109.2 (CH), 101.5 (CH), 56.1 (CH_3), 56.0 (CH_3), 51.4 (CH_3), 21.7 (CH_3). IR (film)ν: 1730, 1597, 1514, 1438, 1267, 1166, 1024, 813, 765 cm^{-1}. ESI-HRMS Calcd for (M + H^+) $C_{20}H_{22}N_2NaO_4S$ 441.1091, found 441.1091.

*4.2.1.15. Methyl (Z)-3-(2-((E)-naphthalen-2-ylmethylene)-1-tosylhydrazinyl) acrylate (**8Z**).* Colourless oil. ^{1}H NMR (300 MHz, $CDCl_3$): δ 8.43 (s, 1H, C4–H), 8.01 (s, 1H, H_{arom}), 7.87- 7.84 (m, 4H, H_{arom}), 7.76 (d, *J* = 8.3 Hz, 2H, C5–H), 7.56-7.53 (m, 2H, H_{arom}), 7.31 (d, *J* = 8.1 Hz, 2H, C6–H), 6.61 (d, *J* = 9.3 Hz, 1H, C3–H), 6.65 (d, *J* = 9.3 Hz, 1H, C2–H), 3.56 (s, 3H, OCH_3), 2.42 (s, 3H, Ts-CH_3). ^{13}C NMR (75 MHz, $CDCl_3$): δ 165.6 (C), 159.0 (CH), 144.9 (C), 134.9 (C), 134.2 (C), 133.4 (CH), 133.0 (C), 131.1 (CH), 130.8 (CH), 129.7 (CH), 128.8 (CH), 128.3 (CH), 127.9 (CH), 127.7 (CH), 126.8 (CH), 122.9 (CH), 112.6 (CH), 51.7 (CH_3), 21.7 (CH_3). IR (film) υ: 1712, 1625, 1371, 1170, 1145, 1087, 813, 704 cm^{-1}. ESI-HRMS Calcd for (M + H^+) $C_{22}H_{20}N_2O_4S$ 409.1217, found 409.1217.

*4.2.1.16. Methyl (E)-3-(2-((E)-naphthalen-2-ylmethylene)-1-tosylhydrazinyl) acrylate (**8E**).* White solid. Mp = 146.2–147.0 °C. ^{1}H NMR (300 MHz, $CDCl_3$): δ 8.85 (s, 1H, C4–H), 8.16 (d, *J* = 13.4 Hz, 1H, C3–H), 8.14 (s, 1H, H_{arom}), 7.96- 7.85 (m, 4H, H_{arom}), 7.68 (d, *J* = 8.4 Hz, 2H, C5–H), 7.58 (quint, J_1 = 5.9 Hz, J_2 = 1.2 Hz, 2H, H_{arom}), 7.32 (d, *J* = 8.4 Hz, 2H, C6–H), 5.44 (d, *J* = 13.5 Hz, 1H, C2–H), 3.72 (s, 3H, OCH_3), 2.43 (s, 3H, Ts-CH_3). ^{13}C NMR (75 MHz, $CDCl_3$): δ 169.1 (CH), 167.3 (C), 145.3 (C), 141.8 (CHx2), 135.5 (C), 133.7 (C), 132.8 (CH), 132.6 (C), 130.0 (CH), 129.0 (CHx2), 128.4 (CH), 128.0 (CH), 127.1 (CH), 123.1 (CH), 102.0 (CH), 51.4 (CH_3), 21.7 (CH_3). IR (KBr) υ: 1712, 1625, 1371, 1170, 1145, 1087, 813, 704 cm^{-1}. ESI-HRMS Calcd for (M + H^+) $C_{22}H_{20}N_2O_4S$ 409.1217, found 409.1217.

*4.2.1.17. Methyl (E)-3-(2-((E)-(1H-pyrrol-2-yl)methylene)-1-tosylhydrazinyl)acrylate (**9E**).* Colourless oil. ^{1}H NMR (300 MHz, $CDCl_3$): δ 8.42 (s, 1H, C4–H), 8.12 (d, *J* = 13.5 Hz, 1H, C3–H), 7.63 (d, *J* = 8.3 Hz, 2H, C5–H), 7.30 (d, *J* = 8.1 Hz, 2H, C6–H), 7.01 (s, 1H, H_{arom}), 6.78 (s, 1H, H_{arom}), 6.35 (s, 1H, H_{arom}), 5.25 (d, *J* = 13.5 Hz, 1H, C2–H), 3.69 (s, 3H, OCH_3), 2.42 (s, 3H, Ts-CH_3). ^{13}C NMR (75 MHz, $CDCl_3$): δ 167.4 (C), 160.6 (CH), 145.1 (C), 142.1 (CH), 133.7 (C), 129.9 (CH), 128.0 (CH), 125.7 (C), 124.8 (CH), 120.0 (CH), 111.4 (CH), 101.0 (CH), 51.4 (CH_3), 21.7 (CH_3). IR (film) υ:1699, 1597, 1436, 1369, 1168, 1087, 1037, 813, 748 cm^{-1}. ESI- HRMS Calcd for (M + Na^+) $C_{16}H_{17}N_3NaO_4S$ 370.0832, found 370.0832.

*4.2.1.18. Methyl (Z)-3-(2-((E)-furan-2-ylmethylene)-1-tosylhydrazinyl) acrylate (**10Z**).* White solid. MP: 102.1–102.9 °C. ^{1}HNMR (300 MHz, $CDCl_3$): δ 8.23 (s, 1H, C4–H), 7.71 (d, *J* = 8.4 Hz, 2H, C5–H), 7.55 (s, 1H, H_{arom}), 7.31 (d, *J* = 8.1 Hz, 2H, C6–H), 6.89 (d, *J* = 3.5 Hz, 1H, H_{arom}), 6.61 (d, *J* = 9.4 Hz, 1H, C3–H), 6.53 (q, J_1 = 3.4 Hz, J_2 = 1.8 Hz, *1H, H_{arom}),* 5.54 (d, *J* = 13.5 Hz, 1H, C2–H), 3.58 (s, 3H, OCH_3), 2.41 (s, 3H, Ts-CH_3). ^{13}C NMR (75 MHz, $CDCl_3$): δ 165.4 (C), 150.1 (CH), 148.5 (C), 145.9 (C), 145.0 (CH), 133.9 (C), 133.8 (CH), 129.8 (CH), 128.2 (CH), 116.7 (CH), 112.2 (CH), 111.3 (CH), 51.5 (CH_3), 21.6 (CH_3). IR (KBr) υ: 2951, 2096, 1712, 1643, 1471, 1435, 1371, 1130, 1087, 937, 661 cm^{-1}. ESI-HRMS Calc for (M + H^+) $C_{16}H_{17}N_2O_5S$ 349.0853, found 349.0853.

*4.2.1.19. Methyl (E)-3-(2-((E)-furan-2-ylmethylene)-1-tosylhydrazinyl) acrylate (**10E**).* Colourless oil. ^{1}H NMR (300 MHz, $CDCl_3$): δ 8.52 (s, 1H, C4–H), 8.09 (d, *J* = 13.5 Hz, 1H, C3–H), 7.65 (d, *J* = 8.6 Hz, 2H, C5–H), 7.64 (s, 1H, H_{arom}), 7.31 (d, *J* = 8.2 Hz, 2H, C6–H), 7.05 (d, *J* = 3.6 Hz, 1H, H_{arom}), 6.59 (q, J_1 = 13.5 Hz, J_2 = 13.5 Hz, 1H, H_{arom}), 5.38 (d, *J* = 13.5 Hz, 1H, C2–H), 3.70 (s, 3H,

OCH_3), 2.42 (s, 3H, Ts-CH_3). ^{13}C NMR (75 MHz, $CDCl_3$): δ 163.3 (C), 157.5 (CH), 147.9 (C), 147.2 (CH), 145.4 (C), 141.5 (CH), 133.6 (C), 130.0 (CH), 127.9 (CH), 119.3 (CH), 112.6 (CH), 102.0 (CH), 51.4 (CH_3), 21.7 (CH_3). IR (film) υ: 2951, 2096, 1712, 1643, 1471, 1435, 1371, 1130, 1087, 937, 661 cm^{-1}. ESI-HRMS Calcd for (M + H^+) $C_{16}H_{17}N_2O_5S$ 349.0853, found 349.0853.

*4.2.1.20. Methyl (Z)-3-(2-((E)-3-methylbut-2-en-1-ylidene)-1-tosylhydrazinyl)acrylate (**11Z**).* Yellow solid. Mp 90–92 °C.^1H NMR (300 MHz, $CDCl_3$): δ 8.36 (d, *J* = 10.1, 1H, C4–H), 7.66 (d, *J* = 8.4, 2H, C5–H), 7.30 (d, *J* = 8.1, 2H, C6–H), 6.61 (d, *J* = 9.5, 1H, C3–H), 6.00 (d, J_1 = 10.5, 1H, CH), 5.41 (d, J_1 = 9.5, 1H, C2–H), 3.63 (s, 3H, OCH_3), 2.41 (s, 3H, Ts-CH_3), 1.96 (s, 3H, CH_3), 1.93 (s, 3H, CH_3). ^{13}C NMR (75 MHz, $CDCl_3$): δ 165.6 (C), 162.9 (CH), 152.1 (C), 144.7 (C), 134.3 (CH), 134.1 (C), 129.8 (CH), 128.1 (CH), 121.5 (CH), 109.3 (CH), 51.3 (CH_3), 27.1 (CH_3), 21.7 (CH_3), 19.5 (CH_3). IR (KBr) υ: 1712, 1620, 1435, 1369, 1168, 1141, 1087, 839, 705 cm^{-1}. ESI-HRMS Calcd for (M + H^+) $C_{16}H_{21}N_2O_4$ 337.1217, found 337.1217.

*4.2.1.21. Methyl (E)-3-(2-((E)-3-methylbut-2-en-1-ylidene)-1-tosylhydrazinyl) acrylate (**11E**).* White solid. Mp: 123.4–124.3 °C. ^1H NMR (300 MHz, $CDCl_3$): δ 8.55 (d, *J* = 10.4 Hz, 1H, C4–H), 8.05 (d, *J* = 13.6 Hz, 1H, C3–H), 7.64(d, *J* = 8.3 Hz, 2H, C5–H), 7.31 (d, *J* = 8.1 Hz, 2H, C6–H), 6.15 (d, *J* = 10.2 Hz, 1H, CH), 5.21 (d, *J* = 13.6 Hz, 1H, C2–H), 3.68 (s, 3H, OCH_3), 2.41 (s, 3H, Ts-CH_3), 2.00(s, 3H, CH_3), 1.98 (s, 3H, CH_3). ^{13}C NMR (75 MHz, $CDCl_3$): δ 169.7 (CH), 167.4 (C), 155.7 (C), 145.1 (C), 141.8 (CH), 133.7 (C), 129.9 (CH), 127.9 (CH), 121.1 (CH), 101.1 (CH), 51.3 (CH_3), 27.1 (CH_3), 21.7 (CH_3), 19.5 (CH_3). IR (KBr) υ: 1712, 1620, 1435, 1369, 1168, 1141, 1087, 839, 705 cm^{-1}. ESI-HRMS Calcd for (M + H^+) $C_{16}H_{21}N_2O_4$ 337.1217, found 337.1217.

*4.2.1.22. Methyl (Z)-3-(2-((E)-cyclohex-1-en-1-ylmethylene)-1-tosylhydrazinyl)acrylate (**12Z**).* Colourless oil. ^1H NMR (300 MHz, $CDCl_3$): δ 7.88 (s, 1H, C4–H), 7.67 (d, *J* = 8.4 Hz, 2H, C5–H), 7.29 (d, *J* = 8.0 Hz, 2H, C6–H), 6.49 (d, *J* = 9.2 Hz, 1H, C3–H), 6.33 (s, 1H, CH), 5.47 (d, *J* = 9.2 Hz, 1H, C2–H), 3.64 (s, 3H, OCH_3), 2.42 (s, 3H, Ts-CH_3), 2.24 (m, 2H, CH_2), 2.16 (m, 2H, CH_2), 1.64 (m, 4H, CH_2). ^{13}C NMR (75 MHz, $CDCl_3$): δ 165.6 (C), 164.9 (CH), 144.7 (C), 142.5 (CH), 135.3 (C), 134.1 (C), 134.0 (CH), 129.5 (CH), 128.3 (CH), 110.8 (CH), 51.5 (CH_3), 26.4 (CH_2), 23.0 (CH_2), 22.1 (CH_2 x2), 21.6 (CH_3). IR (film) υ: 1714; 1622; 1435; 1371; 1286; 1170; 1087; 813; 669 cm^{-1}. ESI-HRMS Calcd for (M + H^+) $C_{18}H_{23}N_2O_4S$ 363.1373, found 363.1373.

*4.2.1.23. Methyl (E)-3-(2-((E)-cyclohex-1-en-1-ylmethylene)-1-tosylhydrazinyl)acrylate (**12E**).* Colourless oil. ^1H NMR (300 MHz, $CDCl_3$): δ 8.15 (s, 1H, C4–H), 8.04 (d, *J* = 13.4 Hz, 1H, C3–H), 7.63 (d, *J* = 8.4 Hz, 2H, C5–H), 7.30 (d, *J* = 8.2 Hz, 2H, C6–H), 6.47 (s, 1H, CH), 5.20 (d, *J* = 13.6 Hz, 1H, C2–H), 3.68 (s, 3H, OCH_3), 2.41 (s, 3H, Ts-CH_3), 2.30-2.25 (m, 4H, CH_2), 1.67 (m, 4H, CH_2). ^{13}C NMR (75 MHz, $CDCl_3$): δ 173.5 (CH), 157.4 (C), 146.1 (CH), 141.9 (CH), 135.2 (C), 134.6 (C), 133.7 (C), 129.8 (CH), 127.9 (CH), 101.1 (CH), 51.3 (CH_3), 26.6 (CH_2), 23.0 (CH_2), 21.7 (CH_2 x2), 21.5 (CH_3). IR (film) υ: 1714; 1622; 1435; 1371; 1286; 1170; 1087; 813; 669 cm^{-1}. ESI-HRMS Calcd for (M + H^+) $C_{18}H_{23}N_2O_4S$ 363.1373, found 363.1373.

*4.2.1.24. Methyl (Z)-3-(2-((E)-(6,6-dimethylbicyclo[3.1.1]hept-2-en-3-yl)methylene)-1-tosylhydrazinyl)acrylate (**13Z**).* Colourless oil. ^1H NMR (300 MHz, $CDCl_3$): δ 7.99 (s, 1H, C4–H), 7.60 (d, *J* = 8.3 Hz, 2H, C5–H), 7.26 (d, *J* = 8.2 Hz, 2H, C6–H), 6.60 (d, *J* = 9.7 Hz, 1H, C3–H), 6.23 (s, 1H, CH), 5.43 (d, *J* = 9.3 Hz, 1H, C2–H), 3.61 (s, 3H, OCH_3), 2.78 (t, *J* = 5.5 Hz, 1H, CH), 2.49-2.41 (m, 6H), 2.15 (s, 1H, CH), 1.29 (s, 3H, CH_3), 1.12 (d, *J* = 9.2 Hz, 1H, CH_2), 0.76 (s, 3H, Ts-CH_3). ^{13}C NMR (75 MHz, $CDCl_3$): δ 165.5 (C), 162.9 (CH), 145.3 (C), 144.7 (C), 138.3 (CH), 134.3 (CH), 134.0 (C), 129.5 (CH), 128.3 (CH), 109.8 (CH), 51.3 (CH_3), 40.6 (CH), 39.7 (CH), 37.6 (C), 32.8 (CH_2), 30.9 (CH_2), 26.0 (CH_3), 21.6 (CH_3), 21.0 (CH_3). IR (film)υ: 1732, 1614, 1433, 1371, 1257, 1170, 1143, 1001, 734 cm^{-1}. ESI-HRMS Calcd for (M + H^+) $C_{21}H_{27}N_2O_4S$ 403.1686, found 403.1686.

*4.2.1.25. Methyl (E)-3-(2-((E)-(6,6-dimethylbicyclo[3.1.1]hept-2-en-3-yl)methylene)-1-tosylhydrazinyl)acrylate (**13E**).* White solid. Mp: 87.9–88.6 °C. ^1H NMR (300 MHz, $CDCl_3$): δ 8.24 (s, 1H, C4–H), 8.06 (d, *J* = 13.6 Hz, 1H, C3–H), 7.58 (d, *J* = 8.5 Hz, 2H, C5–H), 7.29 (d, *J* = 8.0 Hz, 2H, C6–H), 6.39 (s, 1H, CH), 5.20 (d, *J* = 13.6 Hz, 1H, C2–H), 3.69 (s, 3H, OCH_3), 2.87 (t, *J* = 5.1 Hz, 1H, CH), 2.55-2.42 (m, 6H), 2.19 (s, 1H, CH), 1.32 (s, 3H, CH_3), 1.17 (d, *J* = 9.2 Hz, 1H, CH), 0.81 (s, 3H, CH_3). ^{13}C NMR (75 MHz, $CDCl_3$): δ 170.2 (CH), 167.4 (C), 165.4 (C), 145.4 (C), 141.9 (CH), 141.9 (CH), 133.7 (C), 129.8 (CH), 128.0 (CH), 101.2 (CH), 52.6 (CH_3), 40.5 (CH), 39.7 (CH), 37.7 (C), 33.1 (CH_2), 30.9 (CH_2), 25.8 (CH_3), 21.7 (CH_3), 21.0 (CH_3). IR (KBr) υ: 1732, 1614, 1433, 1371, 1257, 1170, 1143, 1001, 734 cm^{-1}. ESI-HRMS Calcd for (M + H^+) $C_{21}H_{27}N_2O_4S$ 403.1686, found 403.1686.

*4.2.1.26. Methyl (Z)-3-(2-((1E,2E,4E)-hexa-2,4-dien-1-ylidene)-1-tosylhydrazinyl) acrylate (**14Z**).* Colourless oil. ^1H NMR (300 MHz, $CDCl_3$): δ 7.99 (d, *J* = 9.6 Hz, 1H, C4–H), 7.67 (d, *J* = 8.2 Hz, 2H, C5–H), 7.29 (d, *J* = 8.2 Hz, 2H, C6–H), 6.69 (dd, J_1 = 15.5 Hz, J_2 = 10.3 Hz, 1H, CH), 6.53 (d, *J* = 9.4 Hz, 1H, C3–H), 6.21 (dd, J_1 = 15.5 Hz, J_2 = 10.3 Hz, 2H, CH), 6.03 (dd, J_1 = 15.0 Hz, J_2 = 6.6H, 1H, CH), 5.49 (d, *J* = 9.4 Hz, 1H, C2–H), 3.64 (s, 3H, OCH_3), 2.41 (s, 3H, Ts-CH_3), 1.85 (d, *J* = 6.9 Hz, 3H, CH_3). ^{13}C NMR (75 MHz, $CDCl_3$): δ 165.4 (C), 163.5 (CH), 144.8 (CH), 144.7 (CH), 137.4 (CH), 134.1 (CH), 133.9 (C), 130.8 (C), 129.7 (CH), 128.2 (CH), 124.9 (CH), 111.1 (CH), 51.6 (CH_3), 21.6 (CH_3), 18.6 (CH_3). IR (film) υ: 1714, 1614, 1435, 1371, 1170, 1145, 1087, 813, 705 cm^{-1}. ESI-HRMS Calcd for (M + H^+) $C_{17}H_{21}N_2O_4S$ 349.1217, found 349.1217.

*4.2.1.27. Methyl (E)-3-(2-((1E,2E,4E)-hexa-2,4-dien-1-ylidene)-1-tosylhydrazinyl) acrylate (**14E**).* Colourless oil. ^1H NMR (300 MHz, $CDCl_3$): δ 8.27 (d, *J* = 9.9 Hz, 1H, C4–H), 8.06 (d, *J* = 13.8 Hz, 1H, C3–H), 7.63 (d, *J* = 8.3 Hz, 2H, C5–H), 7.30 (d, *J* = 8.3 Hz, 2H, C6–H), 6.83 (dd, J_1 = 15.2 Hz, J_2 = 10.5 Hz, 1H, CH), 6.34- 6.16 (m, 3H, CH), 5.25 (d, *J* = 13.7 Hz, 1H, C2–H), 3.69 (s, 3H, OCH_3), 2.41 (s, 3H, Ts-CH_3), 1.89 (d, *J* = 6.3 Hz, 3H, CH_3). ^{13}C NMR (75 MHz, $CDCl_3$): δ 172.2 (CH), 167.4 (C), 147.9 (CH), 145.2 (C), 141.7 (CH), 139.5 (CH), 133.7 (C), 130.6 (CH), 130.0 (CH), 129.8 (CH), 124.2 (CH), 101.3 (CH), 51.4 (CH_3), 21.7 (CH_3), 18.8 (CH_3). IR (film) υ: 1714, 1614, 1435, 1371, 1170, 1145, 1087, 813, 705 cm^{-1}. ESI-HRMS Calcd for (M + H^+) $C_{17}H_{21}N_2O_4S$ 349.1217, found 349.1217.

*4.2.1.28. Methyl (Z)-3-(2-((1E,2E)-3-(4-methoxyphenyl)allylidene)-1-tosylhydrazinyl) acrylate (**15Z**).* White solid. Mp: 137.6–138.6 °C. ^1H NMR (300 MHz, $CDCl_3$): δ 8.14 (d, *J* = 9.4 Hz, 1H, C4–H), 7.70 (d, *J* = 8.3 Hz, 2H, H_{arom}), 7.43 (d, *J* = 8.8 Hz, 2H, C5–H), 7.31 (d, *J* = 8.3 Hz, 2H, C6–H), 7.04 (d, *J* = 15.9 Hz, 1H, CH), 6.90 (d, *J* = 8.8 Hz, 2H, H_{arom}), 6.77 (dd, J_1 = 16.1 Hz, J_2 = 9.4 Hz, 1H, CH), 6.57 (d, *J* = 9.2 Hz, 1H, C3–H), 5.52 (d, *J* = 9.2 Hz, 1H, C2–H), 3.84 (s, 3H, OCH_3), 3.65 (s, 3H, OCH_3), 2.42 (s, 3H, Ts-CH_3). ^{13}C NMR (75 MHz, $CDCl_3$): δ 165.4 (C), 163.8 (CH), 161.0 (C), 144.8 (CH), 144.1 (C), 134.1 (CH), 134.0 (C), 129.7 (CH), 129.2 (CH), 128.2 (CH), 128.1 (C), 121.6 (CH), 114.4 (CH), 111.0 (CH), 55.4 (CH_3), 51.6 (CH_3), 21.6 (CH_3). IR (KBr) υ: 1714, 1602, 1579, 1510, 1438, 1359, 1305, 1257, 1170, 1087, 1028, 819, 738, 661, 597 cm^{-1}. ESI-HRMS Calcd for (M + H^+) $C_{21}H_{23}N_2O_5S$ 415.1322, found 415.1322.

*4.2.1.29. Methyl (Z)-3-(2-((1E,2E)-3-(4-methoxyphenyl)allylidene)-1-tosylhydrazinyl) acrylate (**15E**).* Yellow oil. NMR (300 MHz, $CDCl_3$): δ 8.41 (d, *J* = 9.7 Hz, 1H, C4–H), 8.10 (d, *J* = 13.6 Hz, 1H, C3–H), 7.66 (d, *J* = 8.4 Hz, 2H, C5–H), 7.48 (d, *J* = 8.7 Hz, 2H, H_{arom}), 7.31 (d, *J* = 8.2 Hz, 2H, C6–H), 7.18 (d, *J* = 15.9 Hz, 1H, CH), 6.93 (d,

J = 8.80 Hz, 2H, H_{arom}), 6.88 (dd, J_1 = 16.3 Hz, J_2 = 9.7 Hz, 1H, CH), 5.29 (d, J = 13.6 Hz, 1H, C2−H), 3.86 (s, 3H, OCH_3), 3.70 (s, 3H, OCH_3), 2.42 (s, 3H, Ts-CH_3). ^{13}C NMR (75 MHz, $CDCl_3$): δ 172.4 (CH), 167.4 (C), 161.6 (C), 147.3 (CH), 145.2 (C), 141.8 (CH), 138.1 (C), 133.7 (C), 130.0 (CH), 129.6 (CH), 127.9 (CH), 120.7 (CH), 114.5 (CH), 101.3 (CH) 55.4 (CH_3), 51.4 (CH_3), 21.7 (CH_3). IR (KBr) υ: 1714, 1602, 1579, 1510, 1438, 1359, 1305, 1257, 1170, 1087, 1028, 819, 738, 661, 597 cm^{-1}. ESI-HRMS Calcd for (M + H^+) $C_{21}H_{23}N_2O_5S$ 415.1322, found 415.1322.

4.3. Biology

4.3.1. Bacterial strains

M. tuberculosis strain H37Rv was kindly provided by Dr. L. Barrera (Instituto Nacional de Microbiología "C.G. Malbrán", Argentina). *M. tuberculosis* strain H37Rv InhA-OE was generated in the laboratory of one of us (HRM) [42]. All the mycobacterial strains were routinely grown in Middlebrook 7H9 broth (Difco Laboratories, Detroit, MI, USA) supplemented with 1/10 v/v of ADS (50 g/L BSA fraction V, 20 g/L dextrose and 8.1 g/L NaCl), glycerol (1% w/v). Tween 80 was added to prevent clumping (0.05% w/v). This medium was designated as 7H9-ADS-Gly for short. When needed, solid media Middlebrook 7H11 supplemented with ADS (1/10 v/v) and glycerol (1% v/v) was used. All strains were grown at 37 °C under gentle agitation.

4.3.2. In vitro compound activity against M. tuberculosis (Mtb) strains

Stock solutions for all the tested compounds were made in DMSO at 40 mM. Working solutions were made by dilution in the above described 7H9 - ADS-G medium at a final concentration of 400 μM. Antimycobacterial activity was determined by two-fold dilution of the compounds in Middlebrook 7H9-ADS-G medium as described previously [58]. For this purpose, 96-well plates (Falcon, Cat number 3072, Becton Dickinson, Lincoln Park, NJ) were used. The 96 well-plates received 100 μL of Middlebrook 7H9 broth and a serial two-fold dilution of the compounds was made directly on the plate. The initial and final drug concentrations tested were 20 μM and 1.25 μM, respectively. Four compounds were tested in duplicate in each microtiter plate, Rifampicin (final concentrations ranging from 2 μg/mL to 0.16 mg/mL; stock solution prepared as a 10 mg/mL solution in methanol) was used as control drug. The inoculum was prepared as a 1/25 dilution of a fresh mid-log *M. tuberculosis* H37Rv suspension (O.D equivalent to Mc Farland 1.0 scale value) made in Middlebrook 7H9-ADS-G. A 100 μL aliquot (containing approximately 10^6 Colony Forming Units) was used to inoculate the wells. Plates were sealed with Parafilm and incubated at 37 °C for five days. Minimum Inhibitory Concentration (MIC) was defined as the lowest drug concentration preventing mycobacterial growth displayed as turbidity in the wells.

4.3.3. Cytotoxicity assay

The in vitro cytotoxicity was determined against mammalian kidney fibroblasts (VERO). The assay was performed in 96-well tissue culture-treated plates as described earlier [59]. Briefly, cells were seeded to the wells of the plate (25,000 cells/well) and incubated for 24 h. Samples were added, and plates were again incubated for 48 h. The number of viable cells was determined by neutral red assay. IC_{50} values were determined from logarithmic graphs of growth inhibition versus concentration. Doxorubicin was used as a positive control (IC_{50} = 14 mM, Vero cells), while DMSO was used as vehicle control.

4.4. Docking studies

The receptor structure (PDBID 4TRO) was manually checked, and protonation states were manually assigned using Maestro [60]. Docking calculations were made with AutoDock4 using a pharmacophoric bias [61] on an aromatic interaction between Phe 149 and various ligands computed with an in house script using PyMOL [62] (PDB ids 2B35 2IDZ 2IE0 2IEB 2NTJ 2NV6 2PR2 2X22 2X23 4OHU 4OIM 4OXK 4OXN 4OXY 4OYR 2IDZ 4BQP 2NV6 2X22 2X23 3FNE 3FNF 3FNG 4BQP 4BQR 4COD 4TZK 4U0K 5COQ 5CP8). 100 different runs were used, and the results were clustered while keeping the lowest energy cluster with at least 20% population. After picking the lowest energy conformer a minimization with AMBER 99SB + parm@Frosst [63] for 1000 cycles using Sander 16 from AmberTools [64]. Visualization was performed with VMD [65].

Declaration of competing interest

The authors declare that they have no known competing financial interests or personal relationships that could have appeared to influence the work reported in this paper.

Acknowledgments

This work was supported in part by grants from National Research Council of Argentina, CONICET (2012-14/0448); Agencia Nacional de Promoción Científica y Tecnológica, ANPCyT- Argentina (PICT 2011/0589 to GRL and PICT 2005/38198 to HRM), Universidad Nacional de Rosario (BIO503) and Fundación Josefina Prats. AT, AB, GRL and LAD are members of the scientific staff of CONICET-Argentina. HRM is a career member of CIUNR-Argentina. DGG and ARB thanks CONICET for the award of a fellowship.

Appendix A. Supplementary data

Supplementary data to this article can be found online at https://doi.org/10.1016/j.ejmech.2020.112699.

References

[1] W.H.O., Global Tuberculosis Report, 2015.
[2] J.M. Altimari, S.C. Hockey, H.I. Boshoff, A. Sajid, L.C. Henderson, Novel 1,4-substituted-1,2,3-triazoles as antitubercular agents, ChemMedChem (2015) 787−791.
[3] B.-T. Nyang'wa, C. Berry, K. Fielding, A.J. Nunn, Multidrug-resistant tuberculosis, Lancet 394 (2019) 298−299.
[4] S.K. Parida, R. Axelsson-Robertson, M.V. Rao, N. Singh, I. Master, A. Lutckii, S. Keshavjee, J. Andersson, A. Zumla, M. Maeurer, Totally drug-resistant tuberculosis and adjunct therapies 277 (2015) 388−405.
[5] V. Ramappa, G.P. Aithal, Hepatotoxicity related to anti-tuberculosis drugs: mechanisms and management, J. Clin. Exp. Hepatol. 3 (2013) 37−49.
[6] D. Canetti, N. Riccardi, M. Martini, S. Villa, A. Di Biagio, L. Codecasa, A. Castagna, I. Barberis, V. Gazzaniga, G. Besozzi, HIV and tuberculosis: the paradox of dual illnesses and the challenges of their fighting in the history, Tuberculosis 122 (2020) 101921.
[7] J. Bernstein, W.A. Lott, B.A. Steinberg, H.L. Yale, Chemotherapy of experimental tuberculosis. V. Isonicotinic acid hydrazide (nydrazid) and related compounds, Am. Rev. Tubercul. 65 (1952) 357−364.
[8] N. Simone, M.S. Elizabeth, K. Marisa, M.W. Robin, D.V.H. Paul, Isoniazid resistance and dosage as treatment for patients with tuberculosis, Curr. Drug Metabol. 18 (2017) 1030−1039.
[9] C. Vilcheze, W.R. Jacobs Jr., The isoniazid paradigm of killing, resistance, and persistence in *Mycobacterium tuberculosis*, J. Mol. Biol. 431 (2019) 3450−3461.
[10] C. Vilchèze, J. William, R. Jacobs, The mechanism of isoniazid killing: clarity through the scope of genetics, Annu. Rev. Microbiol. 61 (2007) 35−50.
[11] C. Vilchèze, H.R. Morbidoni, T.R. Weisbrod, H. Iwamoto, M. Kuo, J.C. Sacchettini, W.R. Jacobs, Inactivation of the inhA-encoded Fatty Acid Synthase II (FASII) enoyl-acyl carrier protein reductase induces accumulation of the fasi end products and cell lysis of *Mycobacterium smegmatis*, J. Bacteriol. 182 (2000) 4059−4067.
[12] U. Theuretzbacher, S. Gottwalt, P. Beyer, M. Butler, L. Czaplewski, C. Lienhardt, L. Moja, M. Paul, S. Paulin, J.H. Rex, L.L. Silver, M. Spigelman, G.E. Thwaites, J.-

P. Paccaud, S. Harbarth, Analysis of the clinical antibacterial and antituberculosis pipeline, Lancet Infect. Dis. 19 (2019) e40–e50.
[13] I. Jeong, J.S. Park, Y.J. Cho, H.I. Yoon, J. Song, C.T. Lee, J.H. Lee, Drug-induced hepatotoxicity of anti-tuberculosis drugs and their serum levels, J. Kor. Med. Sci. 30 (2015) 167–172.
[14] X. He, A. Alian, R. Stroud, P.R. Ortiz de Montellano, Pyrrolidine carboxamides as a novel class of inhibitors of enoyl acyl carrier protein reductase from *Mycobacterium tuberculosis*, J. Med. Chem. 49 (2006) 6308–6323.
[15] M.O. Rodrigues, J.B. Cantos, C.R.M. D'Oca, K.L. Soares, T.S. Coelho, L.A. Piovesan, D. Russowsky, P.A. da Silva, M.G.M. D'Oca, Synthesis and antimycobacterial activity of isoniazid derivatives from renewable fatty acids, Biorg. Med. Chem. 21 (2013) 6910–6914.
[16] C. Vilcheze, A.D. Baughn, J. Tufariello, L.W. Leung, M. Kuo, C.F. Basler, D. Alland, J.C. Sacchettini, J.S. Freundlich, W.R. Jacobs Jr., Novel inhibitors of InhA efficiently kill *Mycobacterium tuberculosis* under aerobic and anaerobic conditions, Antimicrob. Agents Chemother. 55 (2011) 3889–3898.
[17] R. Maccari, R. Ottanà, M.G. Vigorita, In vitro advanced antimycobacterial screening of isoniazid-related hydrazones, hydrazides and cyanoboranes: Part 14, Bioorg. Med. Chem. Lett 15 (2005) 2509–2513.
[18] F.C. Santos, H. Castro, M. Lourenço, P. Abreu, P. Batalha, A. Cunha, G.L. Carvalho, C. Rodrigues, C. Medeiros, S. Souza, V. Ferreira, M.B.V. Souza, Tuberculosis: finding a new potential antimycobacterium derivative in a aldehyde–arylhydrazone–oxoquinoline series, Curr. Microbiol. 65 (2012) 455–460.
[19] S.A. Bonnett, J. Ollinger, S. Chandrasekera, S. Florio, T. O'Malley, M. Files, J.-A. Jee, J. Ahn, A. Casey, Y. Ovechkina, D. Roberts, A. Korkegian, T. Parish, A target-based whole cell screen approach to identify potential inhibitors of *Mycobacterium tuberculosis* signal peptidase, ACS Infect. Dis. 2 (2016) 893–902.
[20] S.A. Bonnett, D. Dennison, M. Files, A. Bajpai, T. Parish, A class of hydrazones are active against non-replicating *Mycobacterium tuberculosis*, PloS One 13 (2018), e0198059.
[21] S. Siemann, D.P. Evanoff, L. Marrone, A.J. Clarke, T. Viswanatha, G.I. Dmitrienko, N-arylsulfonyl hydrazones as inhibitors of IMP-1 metallo-beta-lactamase, Antimicrob. Agents Chemother. 46 (2002) 2450–2457.
[22] K.N. De Oliveira, M.R.M. Souza, P.C. Sathler, U.O. Magalhães, C.R. Rodrigues, H.C. Castro, P.R. Palm, M. Sarda, P.E. Perotto, S. Cezar, M.A. De Brito, A.S.S.R. Ferreira, L. Mendes Cabral, C. Machado, R.J. Nunes, Sulphonamide and sulphonyl-hydrazone cyclic imide derivatives: antinociceptive activity, molecular modeling and in silico ADMET screening, Arch Pharm. Res. 35 (2012) 1713–1722.
[23] V.N. Badavath, I. Baysal, G. Ucar, B.N. Sinha, V. Jayaprakash, Monoamine oxidase Inhibitory activity of novel pyrazoline analogues: curcumin based design and synthesis, ACS Med. Chem. Lett. 7 (2016) 56–61.
[24] K.N. De Oliveira, P. Costa, J.R. Santin, L. Mazzambani, C. Buerger, C. Mora, R.J. Nunes, M.M. De Souza, Synthesis and antidepressant-like activity evaluation of sulphonamides and sulphonyl-hydrazones, Biorg. Med. Chem. 19 (2011) 4295–4306.
[25] T.B. Fernandes, M.R. Cunha, R.P. Sakata, T.M. Candido, A.R. Baby, M.c.T. Tavares, E.b.G. Barbosa, W.P. Almeida, R. Parise-Filho, Synthesis, molecular modeling, and evaluation of novel sulfonylhydrazones as acetylcholinesterase inhibitors for alzheimer's disease, Arch. Pharm. 350 (2017) 1700163.
[26] M.S. Kabir, O.A. Namjoshi, R. Verma, R. Polanowski, S.M. Krueger, D. Sherman, M.A. Rott, W.R. Schwan, A. Monte, J.M. Cook, A new class of potential antituberculosis agents: synthesis and preliminary evaluation of novel acrylic acid ethyl ester derivatives, Biorg. Med. Chem. 18 (2010) 4178–4186.
[27] A.S. Haythem, S.M. Mohammad, Hybrid drugs as potential combatants against drug-resistant microbes: a review, Curr. Top. Med. Chem. 17 (2017) 895–906.
[28] P. Li, C. Wu, J. Zhao, D.C. Rogness, F. Shi, Synthesis of substituted 1H-indazoles from arynes and hydrazones, J. Org. Chem. 77 (2012) 3149–3158.
[29] L. Crespin, L. Biancalana, T. Morack, D.C. Blakemore, S.V. Ley, One-pot acid-catalyzed ring-opening/cyclization/oxidation of aziridines with n-tosylhydrazones: access to 1,2,4-triazines, Org. Lett. 19 (2017) 1084–1087.
[30] H. Liu, Y. Wei, Novel synthesis of 3,6-disubstituted-1,2,4,5-tetrazine derivatives from hydrazones by using [hydroxyl(tosyloxy)iodo]benzene, Tetrahedron Lett. 54 (2013) 4645–4648.
[31] W. Hao, T. Zhang, M. Cai, Synthesis of H-pyrazolo[5,1-a]isoquinolines via a silver triflate-catalyzed tandem reaction of N′-(2-alkynylbenzylidene)hydrazide with alcohol, Tetrahedron 69 (2013) 9219–9223.
[32] Z.-L. Yuan, Y. Wei, M. Shi, Aza-michael addition reactions of hydrazones with activated alkynes catalyzed by nitrogen-containing organic bases, Eur. J. Org Chem. (2010) 4088–4097, 2010.
[33] S.A. Hashemi, Regioselective synthesis of (E)-3-[2-(arylmethylene)-1-(arylsulfonyl)hydrazino]-2-propenoates via the reaction of arylsulfonyl hydrazones and alkyl propiolates in the presence of triphenylphosphine, Tetrahedron Lett. 53 (2012) 5141–5143.
[34] J.M. Keith, L. Gomez, Exploration of the Mitsunobu reaction with tosyl- and boc-hydrazones as nucleophilic agents, J. Org. Chem. 71 (2006) 7113–7116.
[35] Y. Kong, W. Zhang, M. Tang, H. Wang, N-Alkylation of tosylhydrazones in the presence of triphenylphosphine, Tetrahedron 69 (2013) 7487–7491.
[36] J.R. Fulton, V.K. Aggarwal, J. de Vicente, The use of tosylhydrazone salts as a safe alternative for handling diazo compounds and their applications in organic synthesis, Eur. J. Org Chem. (2005) 1479–1492, 2005.
[37] V.K. Aggarwal, J. de Vicente, R.V. Bonnert, A novel one-pot method for the preparation of pyrazoles by 1,3-dipolar cycloadditions of diazo compounds generated *in situ*, J. Org. Chem. 68 (2003) 5381–5383.
[38] L. Caviedes, J. Delgado, R.H. Gilman, Tetrazolium microplate assay as a rapid and inexpensive colorimetric method for determination of antibiotic susceptibility of *Mycobacterium tuberculosis*, J. Clin. Microbiol. 40 (2002) 1873–1874.
[39] S. Foongladda, D. Roengsanthia, W. Arjrattanakool, C. Chuchottaworn, A. Chaiprasert, S.G. Franzblau, Rapid and simple MTT method for rifampicin and isoniazid susceptibility testing of *Mycobacterium tuberculosis*, Int. J. Tubercul. Lung Dis. 6 (2002) 1118–1122.
[40] S. Ghiya, Y.C. Joshi, Synthesis and antimicrobial evaluation of hydrazones derived from 4-methylbenzenesulfonohydrazide in aqueous medium, Med. Chem. Res. 25 (2016) 970–976.
[41] P.Y. Muller, M.N. Milton, The determination and interpretation of the therapeutic index in drug development, Nat. Rev. Drug Discov. 11 (2012) 751–761.
[42] J.M. Belardinelli, H.R. Morbidoni, Mutations in the essential FAS II beta-hydroxyacyl ACP dehydratase complex confer resistance to thiacetazone in *Mycobacterium tuberculosis* and *Mycobacterium kansasii*, Mol. Microbiol. 86 (2012) 568–579.
[43] U.H. Manjunatha, S.P.S. Rao, R.R. Kondreddi, C.G. Noble, L.R. Camacho, B.H. Tan, S.H. Ng, P.S. Ng, N.L. Ma, S.B. Lakshminarayana, M. Herve, S.W. Barnes, W. Yu, K. Kuhen, F. Blasco, D. Beer, J.R. Walker, P.J. Tonge, R. Glynne, P.W. Smith, T.T. Diagana, Direct inhibitors of InhA are active against *Mycobacterium tuberculosis*, Sci. Transl. Med. 7 (2015), 269ra3.
[44] P.J. Tonge, C. Kisker, R.A. Slayden, Development of modern InhA inhibitors to combat drug resistant strains of *Mycobacterium tuberculosis*, Curr. Top. Med. Chem. 7 (2007) 489–498.
[45] T.J. Sullivan, J.J. Truglio, M.E. Boyne, P. Novichenok, X. Zhang, C.F. Stratton, H.-J. Li, T. Kaur, A. Amin, F. Johnson, R.A. Slayden, C. Kisker, P.J. Tonge, High affinity inha inhibitors with activity against drug-resistant strains of *Mycobacterium tuberculosis*, ACS Chem. Biol. 1 (2006) 43–53.
[46] M. Martínez-Hoyos, E. Perez-Herran, G. Gulten, L. Encinas, D. Álvarez-Gómez, E. Alvarez, S. Ferrer-Bazaga, A. García-Pérez, F. Ortega, I. Angulo-Barturen, J. Rullas-Trincado, D. Blanco Ruano, P. Torres, P. Castañeda, S. Huss, R. Fernández Menéndez, S. González Del Valle, L. Ballell, D. Barros, S. Modha, N. Dhar, F. Signorino-Gelo, J.D. McKinney, J.F. García-Bustos, J.L. Lavandera, J.C. Sacchettini, M.S. Jimenez, N. Martín-Casabona, J. Castro-Pichel, A. Mendoza-Losana, Antitubercular drugs for an old target: GSK693 as a promising InhA direct inhibitor, EBioMedicine 8 (2016) 291–301.
[47] X. He, A. Alian, P.R. Ortiz de Montellano, Inhibition of the *Mycobacterium tuberculosis* enoyl acyl carrier protein reductase InhA by arylamides, Biorg. Med. Chem. 15 (2007) 6649–6658.
[48] Y. Xia, Y. Zhou, D.S. Carter, M.B. McNeil, W. Choi, J. Halladay, P.W. Berry, W. Mao, V. Hernandez, T. O'Malley, A. Korkegian, B. Sunde, L. Flint, L.K. Woolhiser, M.S. Scherman, V. Gruppo, C. Hastings, G.T. Robertson, T.R. Ioerger, J. Sacchettini, P.J. Tonge, A.J. Lenaerts, T. Parish, M. Alley, Discovery of a cofactor-independent inhibitor of *Mycobacterium tuberculosis* InhA, Life Sci. Alliance 1 (2018), e201800025.
[49] C.A. Lipinski, F. Lombardo, B.W. Dominy, P.J. Feeney, Experimental and computational approaches to estimate solubility and permeability in drug discovery and development settings, Adv. Drug Deliv. Rev. 23 (1997) 3–25.
[50] D.F. Veber, S.R. Johnson, H.-Y. Cheng, B.R. Smith, K.W. Ward, K.D. Kopple, Molecular properties that influence the oral bioavailability of drug candidates, J. Med. Chem. 45 (2002) 2615–2623.
[51] M.D. Shultz, Two decades under the influence of the rule of five and the changing properties of approved oral drugs, J. Med. Chem. 62 (2019) 1701–1714.
[52] 20-08-2015, http://www.organic-chemistry.org/prog/peo/26/03/2014: version.2.
[53] A. Gaulton, L.J. Bellis, A.P. Bento, J. Chambers, M. Davies, A. Hersey, Y. Light, S. McGlinchey, D. Michalovich, B. Al-Lazikani, J.P. Overington, ChEMBL: a large-scale bioactivity database for drug discovery, Nucleic Acids Res. (2012) D1100–D1107.
[54] 20-08-2015, http://www.molinspiration.com.v2014.11.
[55] S. Parikh, D.P. Moynihan, G. Xiao, P.J. Tonge, Roles of tyrosine 158 and lysine 165 in the catalytic mechanism of InhA, the enoyl-acp reductase from *Mycobacterium tuberculosis*, Biochemistry 38 (1999) 13623–13634.
[56] D.A. Rozwarski, C. Vilchèze, M. Sugantino, R. Bittman, J.C. Sacchettini, Crystal structure of the *Mycobacterium tuberculosis* enoyl-ACP reductase, InhA, in complex with NAD+ and a c16 fatty acyl substrate, J. Biol. Chem. 274 (1999) 15582–15589.
[57] A.M. Khan, J. Shawon, M.A. Halim, Multiple receptor conformers based molecular docking study of fluorine enhanced ethionamide with mycobacterium enoyl ACP reductase (InhA), J. Mol. Graph. Model. 77 (2017) 386–398.
[58] D.G. Ghiano, A. de la Iglesia, N. Liu, P.J. Tonge, H.R. Morbidoni, G.R. Labadie, Antitubercular activity of 1,2,3-triazolyl fatty acid derivatives, Eur. J. Med. Chem. 125 (2017) 842–852.
[59] H. Babich, E. Borenfreund, Cytotoxicity of T-2 toxin and its metabolites determined with the neutral red cell viability assay, Appl. Environ. Microbiol. 57 (1991) 2101–2103.
[60] S.R. Schrodinger, 4: Maestro, Version 10.4, Schrödinger, LLC, New York, NY, 2015.
[61] J.P. Arcon, C.P. Modenutti, D. Avendano, E.D. Lopez, L.A. Defelipe, F.A. Ambrosio, A.G. Turjanski, S. Forli, M.A. Marti, AutoDock Bias: improving binding mode prediction and virtual screening using known protein-ligand

interactions, Bioinformatics 35 (2019) 3836–3838.
[62] W.L. DeLano, The PyMOL Molecular Graphics System, Delano Scientific, San Carlos, 2002.
[63] C.I. Bayly, D. McKay, J.F. Truchon, Parm@ Frosst Small Molecule Parameters Compatible with AMBER, 2011.
[64] D.A. Case, T.E. Cheatham 3rd, T. Darden, H. Gohlke, R. Luo, K.M. Merz Jr., A. Onufriev, C. Simmerling, B. Wang, R.J. Woods, The Amber biomolecular simulation programs, J. Comput. Chem. 26 (2005) 1668–1688.
[65] W. Humphrey, A. Dalke, K. Schulten, VMD: visual molecular dynamics, J. Mol. Graph. 14 (1996) 33–38.